EXPERIMENTAL INVESTIGATION OF METHANE REFORMER WITH A CONTINUOUS FLOW REACTOR

by

XIAO ZHANG

Presented to the Faculty of the Graduate School of

The University of Texas at Arlington in Partial Fulfillment

of the Requirements

for the Degree of

DOCTOR OF PHILOSOPHY

THE UNIVERSITY OF TEXAS AT ARLINGTON

September 2016

Acknowledgements

Firstly, I would like to express my sincere gratitude to my supervising professor Dr. Brian H. Dennis for his constant support during my Ph.D. study. I am deeply indebted to his patient mentorship, considerable insight and broad knowledge for my research. His meticulous advice for my dissertation greatly helped me make it presentable. I am inspired by his guidance for not only my current research, but also the future career path.

Furthermore, I would also like to truly thank my committee members, Dr. Kent Lawrence, Dr. Bo Ping Wang, Dr. Ratan Kumar, and Dr. Donghyun Shin. Their valuable comments are essential for this dissertation.

Moreover, I would like to thank my colleagues from CFD lab and CREST lab, Dr. Rajeev Kumar, Dr. Rachaneewan Charoenwat, Dr. Wei Han, Dr. Homayon Homayoni, Olivia Choi, and Pawarat Bootpakdeetam for their friendship and assistance. I would also like to special thank Dr. Shreeyukta Singh for her continuous help and advice in chemistry field, and Dr. Wilaiwan Chanmanee for her support in gas chromatograph.

Last but not least, I would like to thank my parents, Mingwei Zhang and Caixia Chu, for their limitless love and countless encouragement throughout my life. I would like to give heartfelt appreciation to my beloved wife, Yin Li, for your selfless love and support. You always accompany me there to share joyful moment or weather difficult times.

September 7th, 2016

Abstract

EXPERIMENTAL INVESTIGATION OF METHANE REFORMER WITH A CONTINUOUS FLOW REACTOR

Xiao Zhang, Ph.D.

The University of Texas at Arlington, 2016

Supervising Professor: Brian H. Dennis

Over the decades, seeking for an alternative energy source has been more and more significant because of increasing demand with rapid industry expansion. Liquid hydrocarbon from Fischer-Tropsch process is considered as an alternative fuel source because the product is considered as subtle for petroleum-derived. Syngas as feedstock for F-T process plays a crucial role in liquid hydrocarbon production. Among several commercial and experiment technologies, the most common technology for syngas production is natural gas reforming. The product from reforming process has proper carbon monoxide/hydrogen ratio for direct application in F-T synthesis. Meanwhile, combined carbon dioxide into reforming reaction has attracted more and more attention in recent studies, which has great potential to help reduce emission of greenhouse gas. However, the

main challenge for reforming process is to maintain reaction for a long period running. In this study, a lab-scale reactor is designed and evaluated to achieve high efficiency for 2 types of reforming reaction, steam reforming and dry reforming.

For this reactor, methane, the main content of natural gas, was used as reactant gas in the reactor for progressive understanding of reforming. The Nickel based catalyst supported by SiO_2 is preloaded and fixed in the catalyst zone of reactor. The selection and preparation for catalyst and support has been discussed in this study. For Steam Methane Reforming reaction, experimental work is conducted under Steam/Carbon ratio from 1 to 4, temperature range from 700℃ to 800℃. Methane is fed to the reactor at flow rate 55 sccm at 1 atm pressure, where experimental conversion data were obtained. The conversion rate of methane is calculated as a standard for evaluation of reactor efficiency. As part of Fischer-Tropsch process, the quality of gas production is evaluated by H_2/CO ratio. The catalyst is examined by XRD and EDAX spectrum for carbon formation test. For Dry Methane Reforming reaction, experiment is conducted under a temperature range from 500° C to 700° C with molar ratio of CH_4/CO_2 1. The total flow rate for mixture gas is 65 sccm. The conversion rates for both methane and carbon dioxide are calculated. The product quality is examined by H_2/CO ratio. The catalyst stability test is conducted in a high carbon intensity with a CO_2/CH_4 ratio 4 at 700° C and total flow rate 65 sccm. The catalyst is separately characterized in 3 different phases by SEM and XRD technology to identify carbon deposition. The results from experiments state that the reactor is able to

convert methane to syngas with high efficiency and high tolerance for carbon deposition at high temperature environment. COMSOL software is applied for reforming reaction process simulation, and the results from simulation support the statement from experiment.

Table of Contents

List of Illustrations

List of Tables

Chapter 1
INTRODUCTION

In this chapter, I first briefly introduce the background of synthesis gas and emission of Carbon Dioxide (CO_2). Then, the methane (CH_4) reforming technology are reviewed. And, a general introduction for catalyst applied in reforming reaction is presented. At the end of this chapter, the research objectives and the outline of this dissertation are also listed in this chapter.

1.1 Background Introduction

Synthesis gas (syngas) has been considered as a multi-purpose energy product. It is well known as the feedstock for versatile products, including hydrogen, town gas and transport fuel. Syngas is a mixture gas, and the main compositions of syngas are mostly hydrogen (H_2), carbon monoxide (CO), Carbon Dioxide (CO_2) and Methane (CH_4). The percentage of syngas composition is shown in Table 1.1 for instance.

Table 1.1 Compositions of Operational Synthesis Gas (From Clarke-Energy)

Substance	Composition (%)
H_2	20-40
CO	35-40
CO_2	25-35
CH_4	0-15
N_2	2-5

Syngas is widely applied feedstock which could provide service in turbine as heated gas because of heating value, or the utilization of H_2 and CO for a fundamental part of the

downstream fuel chemistry and production applications. Syngas is an important intermediate for the production of synthetic diesel via Fischer-Tropsch process [1]. Conversion Syngas by Fischer-Tropsch process produce an alternative liquid fuel that has some of the most significant benefits for alternative fuels because:

- Reduction in carbon emissions by potential for sequestration of waste gas.
- F-T diesel can be directly use without further engine modification.
- Natural Gas can be guaranteed as long-term primary supply.

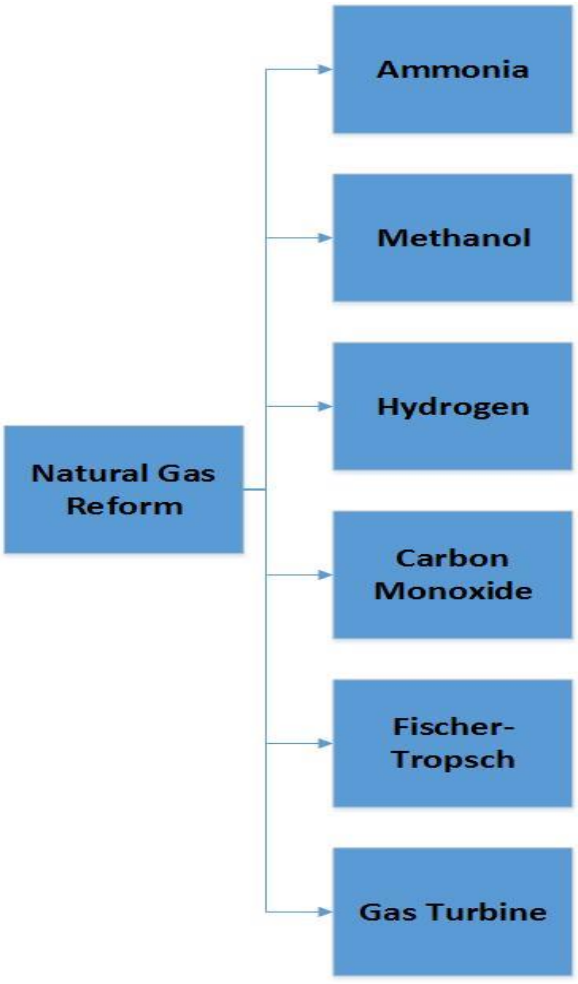

Figure 1.1 Applications of Synthesis Gas

In general, Syngas is a very valuable and versatile product. It can be generally used for vast range of different downstream applications. Therefore, the demand of Syngas, with its value and versatility, would be predominant.

1.2 Emission of Greenhouse Gas

The composition of greenhouse gas include carbon dioxide (CO_2), methane (CH_4), nitrous oxide (NO_2) and fluorinated gases. The distribution of U.S. greenhouse gas emission is showed in Fig 1.2. From this figure, over 90% of greenhouse gas emission is from CO_2 and CH_4. And most of CO_2 comes from electricity production and transportation, which is generated by the combustion of fossil fuel. From Fig 1.2 (c), there are also 29% of CH_4 emissions from natural gas and petroleum systems, which is the largest source of CH_4 emission. Because CH_4 is often found alongside those fossil fuel and relative productions [2].

The fossil fuels, which contain high percentages of carbon, are greatly consumed in both industry and daily life, including power plant, automobile, heating appliance and so on. The CO_2 emission in U.S. from fossil fuels consumption is 5072.3 million metric tons in 2012 [2], which is slightly decreased compared to 2011. But the CO_2 emission still relatively exceed the natural absorption process, which is only 18.2 percent of U.S. CO_2 emissions in 2012 [2]. The rate of greenhouse gas emission has succeeded absorption rate

of earth which leads to continuous increase concentration of greenhouse gas in atmosphere [3]. One of major effect caused by these emissions is deterioration of global warming.

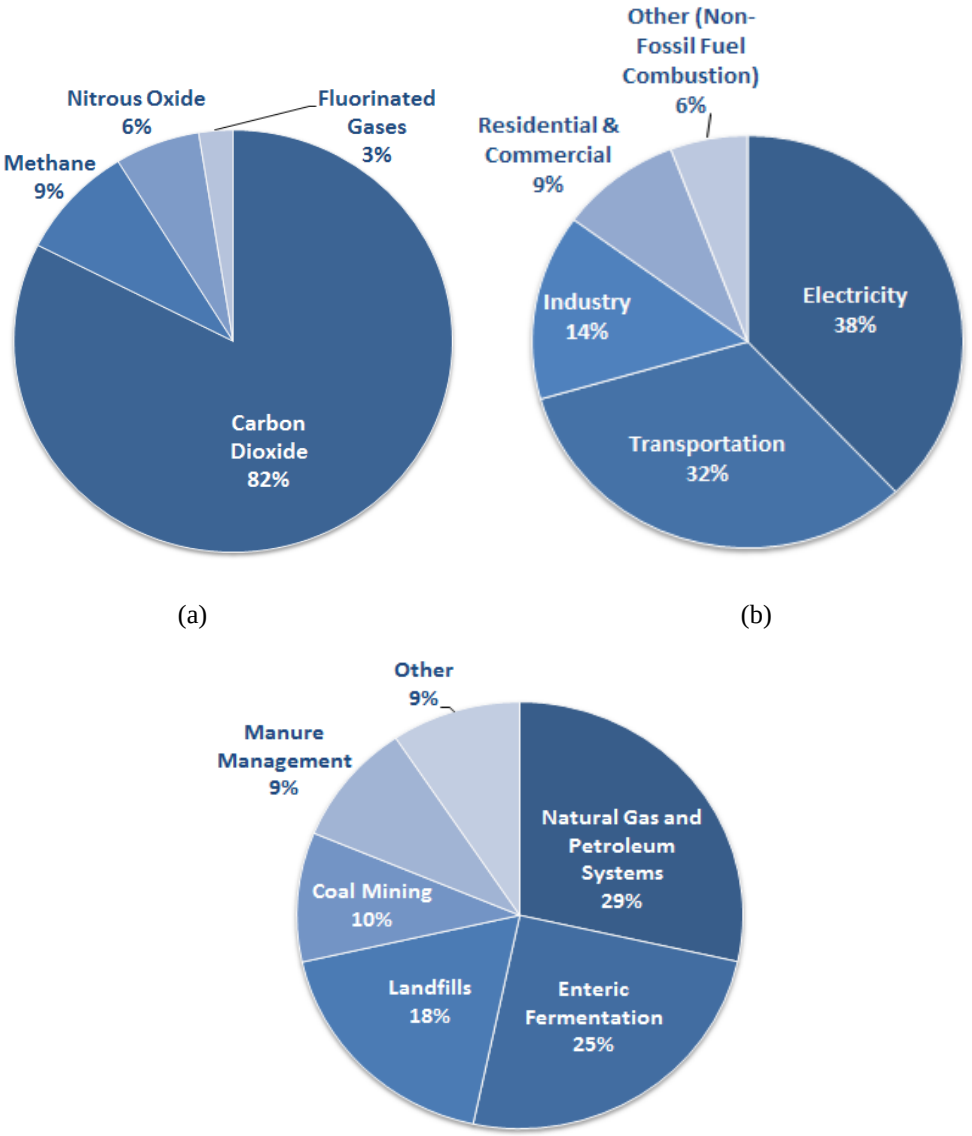

Figure 1.2 (a) U.S. Greenhouse Gas Emissions in 2012 (b) U.S. Carbon Dioxide Emission by Source (c) U.S. Methane Emission by Source

(Source: United States Environmental protection Agency)

Under the pressure of environment and urgent demand of energy, research for recovery and disposal CO_2 has been more and more attracted in recent years. It has been noticed that the great potential of catalytic CH_4-CO_2 reforming would be an effective solution for consuming two major problematic greenhouse gases to produce syngas. Because compared to other conventional fossil fuel, synthetic liquid fuel by Fischer-Tropsch process is a promising alternative due to its capability for the control of greenhouse gas effect.

1.3 Technologies of Syngas Production

Synthesis gas is a mixture gas that contains mainly carbon monoxide, hydrogen and carbon dioxide, and the composition percentage for each gas could be determined by different production processes. Several commercial and experimental technologies are applied for syngas production [4]. Syngas could be produced by coal pyrolysis, biomass gasification [5], and convert from CO_2 and H_2O drove by microwave energy [6] or solar energy [7]. The steam methane reforming is the most common technology in industry [8] and is more suitable for hydrogen, or syngas, production because of more hydrogen concentration in production gas compared to another dominant syngas production process, coal gasification (pyrolysis). Methane as light hydrocarbon contain much more hydrogen than carbon. As shown in Table 1.2, H/C ratio of Methane is the highest among listed materials. Therefore, syngas produced from methane has a higher H2/CO than coal [9]. For

Fischer-Tropsch diesel production, a H_2/CO syngas molar ratio, which is from less than one to over two [10], may be required.

Table 1.2 H/C Atomic Ratio of Typical Feedstock [11]

Materials	H/C
Coke	0.13
Charcoal	0.32
Anthracite	0.38
Bituminous coal	0.80
Lignite	0.86
Peat	1.15
Heavy and residual oil	1.41
Wood	1.44
Crude oil	1.71
Lignite fuel oil	2.00
Naphtha (light distillate feedstock)	2.18
Liquefied petroleum gases (LPG)	2.67
Liquefied nature gases (LNG)	3.43
Methane	4.00

There are several major reforming processes of syngas production:

- Steam Reforming
- Partial Oxidation
    - Thermal Partial Oxidation
    - Catalytic Partial Oxidation
- Autothermal Reforming
- Dry Reforming (CO_2 Reforming)

In general terms, steam methane reforming (SMR) is a thermal process for syngas or hydrogen production under an action of catalyst at high temperature. The major stoichiometry for steam methane reforming is presented in Equation 1.1.

$CH_4 + H_2O \leftrightarrow CO + 3H_2$, $\Delta H = +206$ kJ /mol (1.1)

The excess steam involved in the SMR reaction lead to water gas shift reaction (Eq. 1.2), which helps increase the H_2/CO of product gas.

$CO + H_2O \leftrightarrow CO_2 + H_2$, $\Delta H = -41$ kJ/ mol (1.2)

Therefore, the combination reaction for SMR is:

$CH_4 + 2H_2O \leftrightarrow CO_2 + 4H_2$, $\Delta H = +165$ kJ /mol (1.3)

As indicated by Eq. 1.1, Eq. 1.2, and Eq. 1.3, the steaming reform process is combined by two steps: First, Eq. 1.1 is the reforming reaction which is a strongly endothermic reaction occurred at high temperature; second, Eq. 1.2, water gas shift reaction, is preferred at lower temperature because this reaction is exothermic [12].

Partial oxidation (POX), which is exothermic, is an alternative reforming process to produce syngas. The following equation represent partial oxidation reactions:

$CH_4 + 1/2\ O_2 \leftrightarrow CO + 2H_2$, $\Delta H = -36$ kJ /mol (1.4)

There are three types of POX reaction, thermal partial oxidation (TPOX) with high temperature, catalytic partial oxidation (CPOX) under catalyst action to react at lower temperature, and received heat from autothermal reforming (ATR), which is an exothermic reaction [13]. Partial oxidation (POX) can handle a wide range of feedstock from light

hydrocarbon to heavier petroleum fractions. The temperature range for TPOX is typically from 1200℃ to 1500℃. To activate catalyst, CPOX requires lower temperature around 900℃. The advantage of TPOX over CPOX is that sulfur compound is suspended in the reaction for longer time [12]. Although steam reforming is endothermic reaction required more energy than partial oxidation, the cost of device for oxygen supply and desulfurization process still obstruct the development of partial oxidation.

Autothermal reforming combines the exothermic partial oxidation with endothermic steam reforming reactions in one reactor. In this reaction, fuel, steam and air are feeding into a reactor with catalyst supporting both partial oxidation and steam reforming. The reaction contains 2 parts: one is combustion or partial oxidation area; another is catalytic area. The Eq. 1.6 is a possible oxidation reaction in combustion area. The excess methane will continually consume the steam in catalytic area based on Eq. 1.1 through 1.3.

$CH_4 + 3/2\ O_2 \leftrightarrow CO + 2H_2O,\ \Delta H = -519\ kJ\ /mol$ (1.5)

The heat generated by the oxidation reaction is transferred to compensate steam reforming reaction, which makes temperature low in the reactor [13]. Therefore, the exothermic partial combustion of the fuel can supply heat and steam to methane reforming reactions, the reactor system requires less steam and can be compact and simplified without external heating source [12]. However, unexpected carbon deposition in reactor is always a serious problem causing equipment damage, pressure drop, and poor thermal properties [14].

Dry reforming (CO_2 Reforming) has been broadly mentioned in recent research, since its production of syngas could be desirable feedstock for Fischer-Tropsch synthesis [15]. In addition, CO_2 reforming of CH_4 has important reduction in greenhouse effect by converting CH_4 and CO_2 into value syngas. The reaction for Methane reforming with CO_2 is shown by Eq. 1.6.

$CH_4 + CO_2 \leftrightarrow 2CO + 2H_2$, $\Delta H = +247$ kJ /mol (1.6)

The CO_2 reforming of Methane is an endothermic reaction, which require more energy than convention steam reforming. And coke deposition cause catalyst deactivation is another drawback for CO_2 reforming.

Currently, it is acknowledged that the excellent thermal performance and low cost are the major advantages, which make catalytic steam reforming of natural gas widely adopted in industry scale syngas production [84].

1.4 Catalyst for Reforming

There has been extensive amount of active metal, including noble metals and transition metals, as reforming catalysts. The Methane Steam Reforming is conducted at 850° C, and excess steam is utilized for high S/C ratio range from 2-5 to protect nickel catalyst away from deactivation in industry application [16]. Coke Formation, which leads to catalyst deactivation and structure failure, is extremely harmful for SMR reaction. Lower S/C ratio (< 1.4) and atmospheric pressure are beneficial for coke formation. The most suitable

temperature is at 637˚ C for coke formation [17]. The carbon usually forms at the interface between active metal and the catalyst support with a temperature range of 500–700˚ C. The carbon accumulated on the catalyst will make catalyst failure [18]. Noble metals as catalyst have great performance in prevention of carbon formation, which has specific property to dissolve carbon into these metals [19]. The common noble metal adopted as catalyst are Rhodium, Platinum, Palladium, Ruthenium and Iridium. Noble metals catalysts are stable for methane reforming [20] compared with conventional nickel catalysts. Rh and Ru catalysts totally avoid carbon deposition during reaction, since no carbon is detected. Pd catalyst is able to depress carbon deposition under 650˚ C, and Ir and Pt catalysts can resist carbon deposition under 750˚ C [21]. However, high price and low availability of noble metals limited extensively application as catalyst in industry reforming process [22].

1.5 Research Objectives

In this study, a reactor for two types of methane reforming reaction will be designed and tested as feedstock provider in Fischer-Tropsch synthesis, which is another study in our group. In order to make synthesis gas, which could be used directly in Fischer-Tropsch process, the overall project examines a laboratory-scale fixed-bed reactor to tailor the syngas desirable for downstream process requirement. This reactor has proven to be feasible, archived high natural gas conversion rate and performed excellence in stability

test; on the other hand, the device is remained portable. In addition, experiment devices for the dry reforming process has also been evaluated.

The nickel-based non-precious metal catalyst has been applied because of low cost and metal availability. Nickle Catalyst has been characterized by using XRD and SEM techniques to analyze material's properties and performance. And the mechanical and chemistry properties of catalyst support is greatly effect on the performance of the catalyst in the reaction. Compared to previous research using common Ni/Al_2O_3, the reformer reactor has the potential to help improve reaction effect by using Ni/SiO_2 catalyst.

1.6 Thesis Outlines

Chapter 1 briefly introduces background of syngas and Fischer-Tropsch process. The CO_2 affection for global warming is introduced. And the technology of reforming process for syngas production is presented. The significance of syngas product from reforming is discussed.

Chapter 2 contains literature review and introduction of methodology. The Fischer – Tropsch process is also briefly introduced. The network of reactions for two major reforming methods, CO_2 reforming and steam reforming, are presented. The catalyst selection for reforming process is reviewed based on previous study. The effect of catalytic support is discussed. The catalyst preparation method is discussed, and the process is presented. The technologies of catalyst characterization are also introduced. Gas

Chromatography technique is presented with calibration figures for the single gas component.

Chapter 3 shows the steam methane reforming reactor with nickel catalyst. The concept of reactor design, material, the experimental setup and procedure are described. Meanwhile, the experiment has been investigated by the effect of essential parameters, and the quality of syngas production is evaluated. The characterization of Ni/SiO_2 is also discussed.

Chapter 4 demonstrates the process of CO_2 reforming of CH_4. The investigation on the effects of temperature for production quality is conducted. The Ni catalyst has been characterized by XRD and SEM to compare the different properties in 3 phase, and analysis carbon deposition on the surface. Catalyst duration test for CO_2 reforming of CH_4 is achieved.

Chapter 5 discuss the simulation process for both Steam Reforming and Dry Reforming. The governing equations and kinetic equations for reactions has been presented. The results from simulation has been compared with experiment, and varies parameters are involved in the simulation to predict the reactions for implement. The results for combination of steam reforming and dry reforming has been investigated based on simulation results.

Chapter 6 concludes results for this reactor in 2 kinds of reforming process. The recommendations for future work are summarized.

Chapter 2

LITERATURE REVIEW AND METHDOLOGY

Reforming technologies are broadly applied in industry to produce variety chemicals for downstream processes. In this study, the reforming processes is limited to a specific application, as feedstock provider for Fischer-Tropsch synthesis. For this purpose, two kind of reforming system are setup for desired syngas ratio.

First, the steam methane reformer produces syngas with a high H_2/CO ratio. Second, the syngas with a low H_2/CO ratio is produced from CO_2 reforming with CH_4.

2.1 Fischer-Tropsch Synthesis Process

In 1920s, two German scientists, Franz Fischer and Hans Tropsch, discovered a method to convert syngas into liquid fuel at Kaiser Wilhelm Institute for Coal Research (presently Max Planck Institute for Coal Research) [23]. They performed the reactions over iron catalysts at 400-450 °C and atmospheric pressure to result in a product of liquid fuel. The overall reactions of the Fischer-Tropsch synthesis are listed below based on different products of alkanes, alkenes and alcohols:

$$n\,CO + (2n+1)\,H_2 \rightarrow C_nH_{2n+2} + n\,H_2O \qquad (2.1)$$

$$n\,CO + 2n\,H_2 \rightarrow C_nH_{2n} + nH_2O \qquad (2.2)$$

$$n\,CO + 2n\,H_2 \rightarrow C_nH_{2n+2}O + (n-1)\,H_2O \qquad (2.3)$$

where n is an integer.

Therefore, the component of F-T process is a complex mixture of hydrocarbon and oxygenated products. Since the water is main product from F-T process, the water gas shift reaction (WGS) is also activated under certain conditions.

$CO + H_2O \leftrightarrow CO_2 + H_2$, $\Delta H = -41$ kJ/ mol (2.4)

The common metal catalyst for F-T process are cobalt, iron, ruthenium and nickel. Among them, cobalt and iron are commonly used in industry-scale F-T process at a temperature from 200℃ to 300℃ with a pressure from 10 to 60 bar [24]. Synthetic fuels produced by the F-T process has gained more interest as high quality transportation fuels, which are absence of sulfur, nitrogen and aromatics [25].

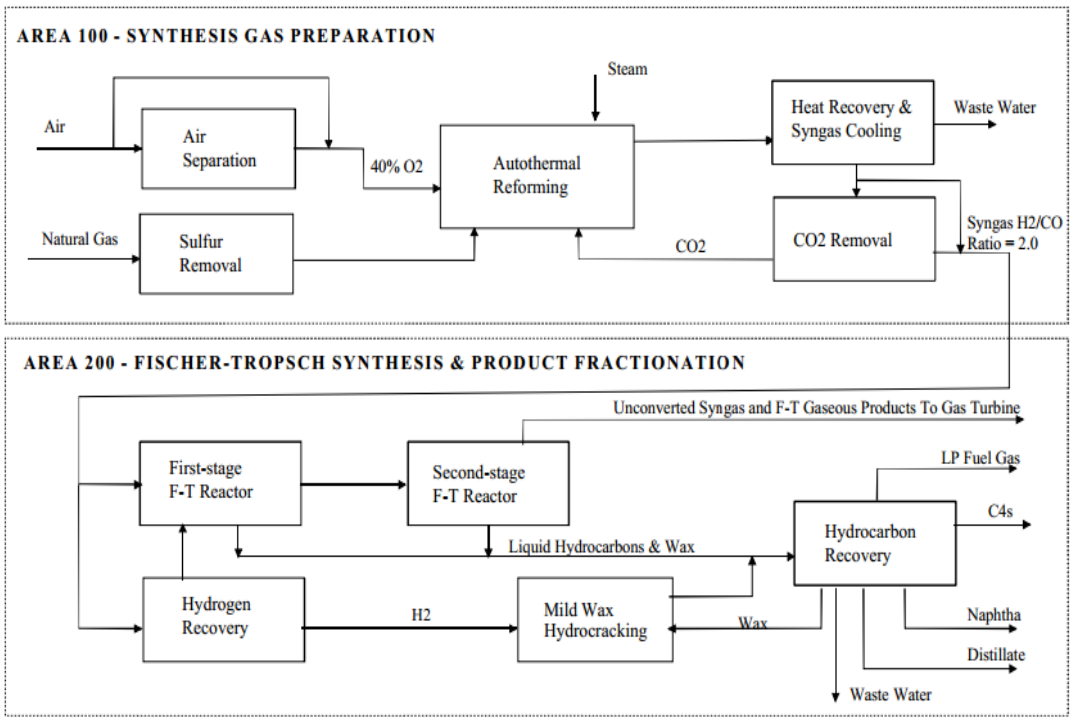

Figure 2.1 Overall process scheme for Fischer- Tropsch Process (taken from [26])

Figure 2.1 shows a Fischer-Tropsch Design flow diagram. In this figure, area 100 part is synthesis gas preparation. From Choi et al. [26] ‘s analysis, the syngas preparation plays a major part in capital cost of F-T process. Hence, to build up an efficient and feasible way for syngas production is our research aim.

2.2 Steam Reforming

Steam reforming process has been broadly used since the 1930s for production of hydrogen or syngas [27]. Methane as a main part of the natural gas, which is naturally stored, is in abundant quantities and cheaper than steam production [28]. Therefore, steam methane reforming is widespread in commercial chemical production. Steam Methane Reforming (SMR) is consist of two major reactions, the endothermic reforming reaction and the weakly exothermic WGS. Desulfurized and pretreated methane from natural gas must be provided to avoid catalyst poisoning.

With methane and superheated steam fed into reactor, the following equations describe collection of possible reactions under steam-reforming conditions:

• Major Reactions

$CH_4 + H_2O \leftrightarrow CO + 3H_2$ (SMR)

$CO + H_2O \leftrightarrow CO_2 + H_2$ (WGS)

• Undesired Reactions including Boudouard reaction, Methane Cracking and Coke Gasification

$2CO \leftrightarrow CO_2 + C$, $\Delta H = -172$ kJ /mol (2.5)

$CH_4 \leftrightarrow C + 2H_2$, $\Delta H = +75$ kJ /mol (2.6)

$C + H_2O \leftrightarrow CO + H_2$, $\Delta H = +131$ kJ /mol (2.7)

The Eq. 2.5 and Eq. 2.6 are very unfavorable because of coke formation, which is harmful for reformer. Therefore, the SMR has to be performed at high temperature and moderate steam-to-carbon ratio (500-900°C and 2.5-3) in order to avoid coke and yield desired hydrocarbon [29].

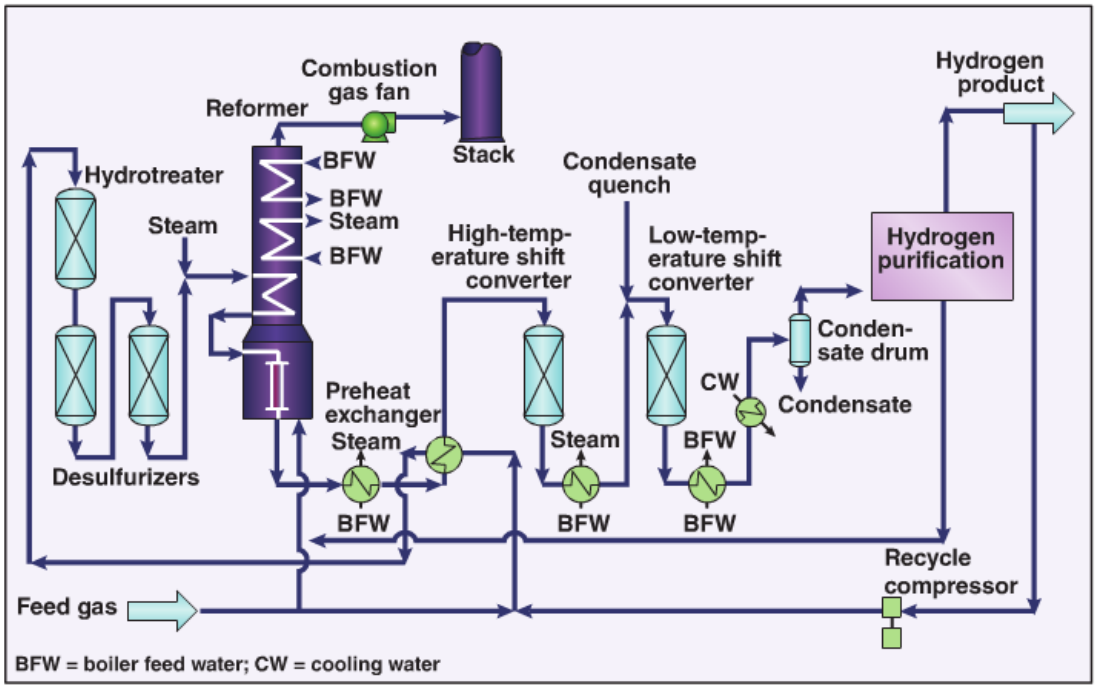

Figure 2.2: Scheme of industrial-scale steam reforming process (taken from [30])

An industry steam methane reforming scheme for hydrogen manufacturing is presented in Figure 2.2. The preheated hydrocarbon feed gas is desulfurized by passing through hydro treater and desulfurizer before flowing into the catalyst reformer. Typically, the reformer

maintains at 760 °C and the steam to hydrocarbon ratio is three [30]. For hydrogen production, the WGS reactors enhance conversion rate to maximize hydrogen production. Then the hydrogen is purified by purification process for downstream applications. Majority of the hydrogen (37%) is as feedstock for ammonia plant with nitrogen [30], but compare to other energy sources, hydrogen, as fuel cell supply, is a promising alternative to fossil fuels due to its clean and non-polluting nature without restriction of location [31].

2.3 Water Gas Shift Reaction

Water Gas Shift (WGS) is an important reaction alongside steam reforming process.

$CO + H_2O \leftrightarrow CO_2 + H_2$

The WGS reaction convert CO into H_2 for increasing concentration of H_2 in product

Because WGS reaction is slightly exothermic, the conversion rate is depressed by increasing temperature. Metal catalyst is also required due to lower reaction rate at a low temperature [32]. This process is reversible, so it is commonly used to tailor ratio of H_2/CO for syngas product. Both forward and reverse reactions will occur at temperature range from 400 °C to 1200 °C [33]. However, the equilibrium constant of reverse WGS reaction is less than 0.1 at high temperature in the results from previous study [33]. The pressure has no effect for WGS reaction's equilibrium, since the volume remain same before and after the reaction.

2.4 CO_2 Reforming

The trend of CO_2 reforming investigation is more and more attractive with increasing environmental issue caused by greenhouse gas and urgent demand of searching alternative fuel. For CO_2 reforming, there is no steam involved in the reaction, so this reaction is also known as dry reforming. The chemical equation of the dry reforming is shown in equation below.

$CH_4 + CO_2 \leftrightarrow 2CO + 2H_2$ (Dry Reforming)

The H_2/CO ratio value of syngas as product of this reaction is 1 from equation, so this syngas production is considered suitable as raw feedstock for the F-T synthesis. However, there are 2 disadvantages for the CO_2 reforming. First, compare to cheap raw materials, CH_4 and CO_2, the cost of amount energy consumption cannot be neglected due to endothermic property of CO_2 reforming. Another one is coke deposition at high temperature with high carbon concentration, which leads to catalyst deactivation and slugging inside the reactor.

2.4.1 CO_2-Steam Mixed Reforming

From above steam reforming and water gas shift reactions, CO_2 is contained in the syngas. Therefore, it can be added into reactor as a complement to adjust the H_2/CO ratio for syngas suitable for downstream process. The simplified flow chart is presented in Fig. 2.3.

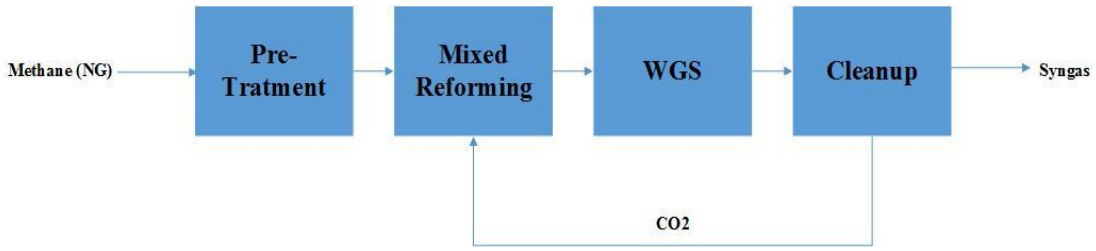

Figure 2.3 Simplified flow chart of CO2-Steam mixed reforming

The O/C and H/C ratio in the feed gas may affect the tendency to carbon deposition [34]. The lower H_2O/CH_4 and H_2/CO ratios is set, the higher coke formation potential [35]. Therefore, in dry reforming, the rich carbon environment leads to a faster carbon formation than steam reforming. By combining CO_2 and Steam together, the coke deposition is controlled.

The process of CO_2-steam mixed reforming has 4 major parts. After pretreatment for feed gas, the steam and CO_2 are mixed in the reformer at high temperatures. Then, after passing through WGS reactor, a cleanup unit is applied to remove CO_2 from product. The pressure swing adsorption technology is usually adopted in CO_2 removal for commercial reforming plant.

2.4.2 Sulfur-Passivated Reforming (SPARG) Process

The sulfur-passivated reforming was designed to produce low H_2/CO ratio syngas by replacing part of steam with CO_2. The first commercialized SPARG plant was built in Texas in 1987 to obtain lower H_2/CO ratio. The previous study showed that the rate of the carbon formation was more sensitive to sulfur than the reforming rate [36]. Therefore, a

sulfur-passivated catalyst, by partially poisoning catalyst with sulfur, is used to decrease the possibility of carbon growth. And the partial poisoned catalyst remains capability to archive high conversion rate. Fig. 2.4 shows a flow chart of SPARG process. The feed gas, steam and CO_2 are mixed in the reactor. The different concentration of CO_2 and steam allows the syngas composition have a low H_2/CO.

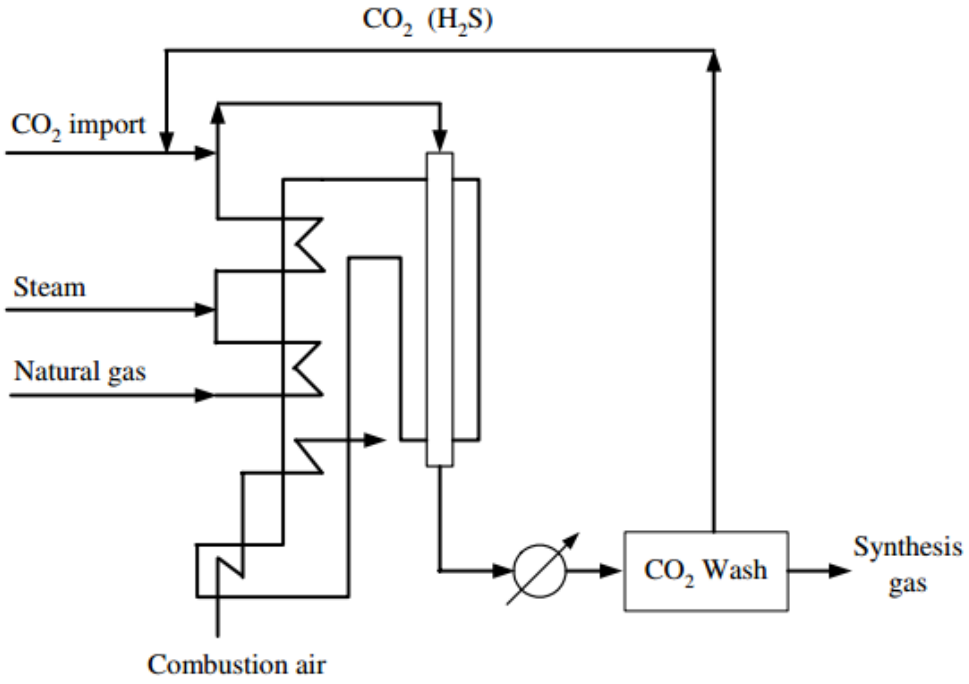

Figure 2.4 Simplified schematic of SPARG process (taken from [37])

2.4.3 CALCOR Process

The CALCOR process aims to produce high purity CO or CO-rich syngas. The CALCOR is operated at a low pressure and a high temperature conditions, which is similar to the dry reforming reaction. The schematic of CALCOR economy process is summarized in Fig. 2.5 from previous work [38]. The feed gas and excess CO_2 is preheated and desulfurized for catalyst protection and H_2 reduction before flowing into reactor. In the reactor, the feed is reformed to mixture syngas. Then the CO in the mixture is purified by 2 membrane stages. And the rest of mixture are recycled for CO_2 recover and combustion fuel for reformer heating process.

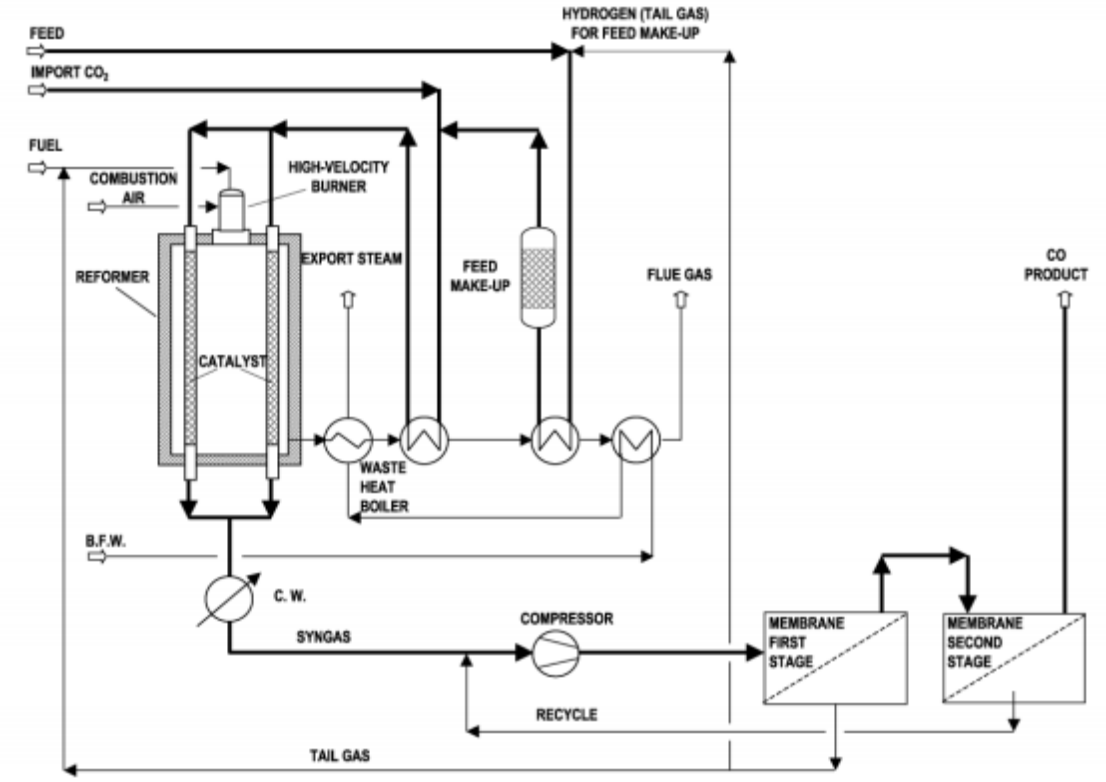

Figure 2.5 Simplified schematic of CALCOR process (taken from [38])

2.5 Coke Formation

Coke formation is a major problem in steam reformers lead to catalyst deactivation. The metal surface of catalyst is covered by carbon deposition, and the reactants cannot contact active catalyst sites leading to deactivation. Meanwhile, coke formation in the reform reactor increase the pressure and block the gas flow. Two main reactions, Methane cracking reaction and Boudouard reaction, are contributed to coke formation during the reforming process.

Methane Cracking $CH_4 \leftrightarrow C + 2H_2$, $\Delta H = +75$ kJ /mol

Boudouard Reaction $2CO \leftrightarrow CO_2 + C$, $\Delta H = -172$ kJ /mol

Methane cracking occurs at high temperature and high pressure, when the Boudouard reaction happen at lower temperature [39]. The feed ratio of S/C is also significant factor for coke formation tendency, because that high coke formation rate is paralleled with low H_2O/CH_4 ratios [35].

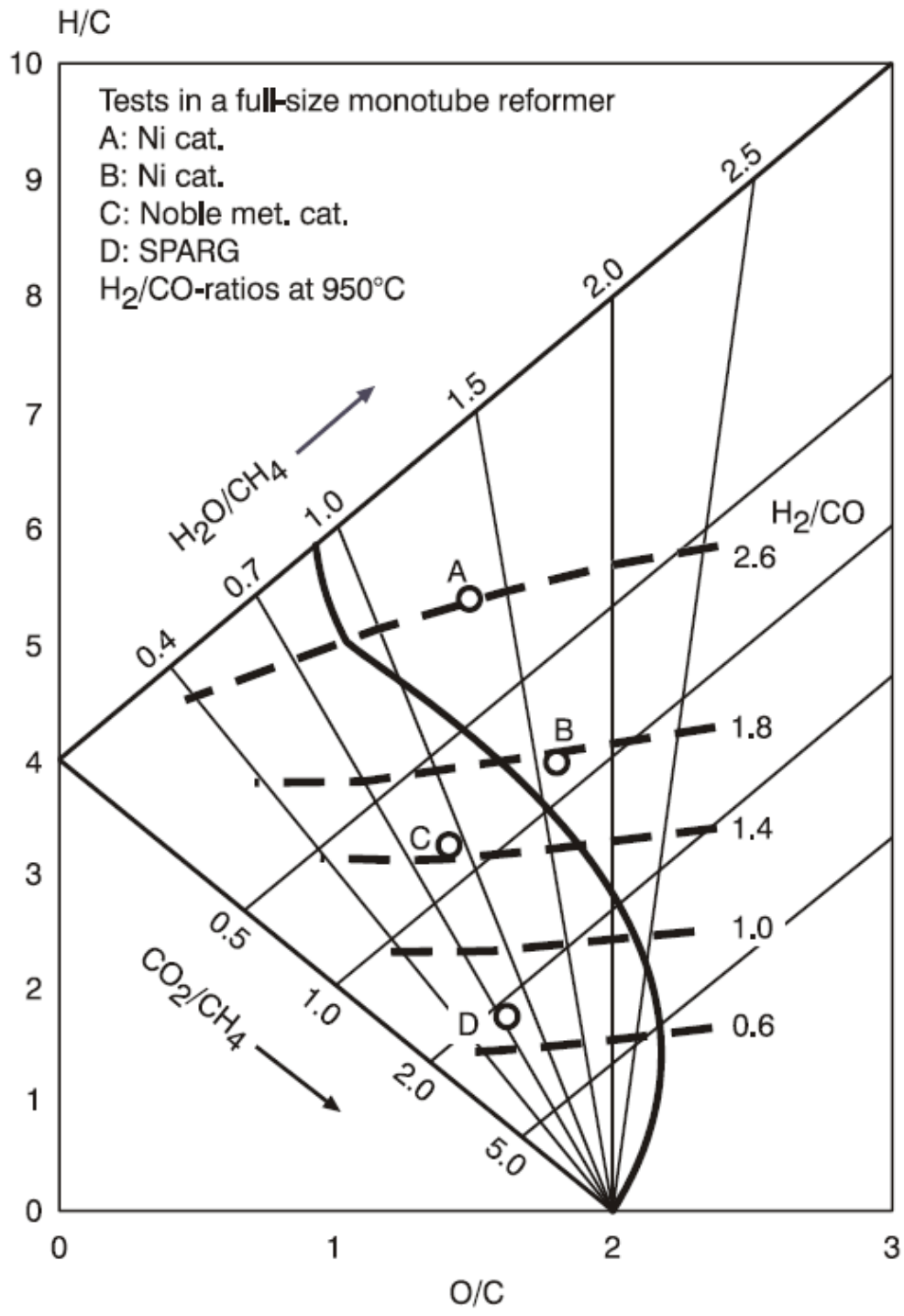

Figure 2.6 Carbon limit diagram. P=25.5 bar (taken from [40])

The diagram limit for carbon limit with different S/C and CO_2/CH_4 ratios is defined in Figure 2.6 [40]. The figure thermodynamically predicated carbon using different molar ratio of CO_2/CH4 and S/C at conditions of 25.5 bar. The mixing ratio to the left limit curve has thermodynamic potential for the carbon formation, while those on the right side of the curve does not. The H_2/CO ratio is indicated by different combinations of S/C and CO_2/CH_4 ratios at the reformer outlet. This carbon limit diagram is for Nickel catalyst. For point C and D, using noble metals and sulfur passivated catalyst is possible to decrease coke formation even in the coke zone for Ni catalyst [40]. Consequently, there are several ways inhibit carbon formation. Combining steam and CO_2 is a possible method to reduce the risk of the coke formation, since steam could increase the H/C ratio. But the H_2/CO ratio will also increase with the addition of water, which cannot be directly applied for Fischer-Tropsch synthesis. Coupling with partial oxidation is an alternative method to increase O/C ratio. And noble metal catalyst is also very helpful for limiting carbon formation. However, the high cost for both of them is not welcome for commercial application. Therefore, the research aim for the future is to establish reforming reaction at conditions in the coke zone, in which locate left to the carbon limit cure, with depressed carbon formation.

2.6 Catalyst

2.6.1 Catalyst Review

The catalyst for Steam Methane Reforming, Dry Reforming, and Partial Oxidation Reforming has been extensively reported in literatures. The performance of various transition and noble metal catalysts involving Rh, Ru, Pt, Pd, and Ni are studied with different supports. Table 2.1 presents the various catalyst has been investigated over different support.

Table 2.1 Metal catalysts with different support for Syngas/H_2

Catalyst Metal	Support	Reaction	Ref.
Pt	Al_2O_3	SRM	[41][55]
Pt	ZrO_2	SRM	[41][54][55]
Pt	ZrO_2-CeO_2	SRM	[41]
Rh	Al_2O_3	Dry/SRM	[42-45][47]
Rh	ZrO_2	Dry/SRM	[42-43]
Rh	SiO_2	Dry	[42][45][47]
Rh	MgO	Dry	[45-47]
Ir	MgO	Dry	[46]
Ir	CeO_2	SRM/POX	[56]
Ir	Al_2O_3	Dry	[57]
Ni	$MgAl_2O_4$	SRM	[40][48]
Ni	Al_2O_3	Dry	[49-50][53][63]
Ni	MgO-SiO_2	Dry	[51]

Ni	MgO	Dry	[52]
Ni	SiO_2	Dry	[62-63]
Pd	ZnO	SR of Methanol	[58-59]
Pd	γ-Al_2O_3	SR of Ethanol	[60]
Pd	CeO_2	SRM	[61]
Ru	Al_2O_3	SR of ethanol	[64][66]
Ru	MgO	SRM	[65]
Ru	TiO_2	Dry	[66]

(SRM: Steam Methane Reforming, SR: Steam Reforming, Dry: CO_2 Reforming for Methane, POX: Partial Oxidation Reforming)

In general, the catalytic activity of metal catalysts is following the order: Ru> Rh> Ir> Pd> Pt> Ni. Thus, these noble metals as catalyst in the processes of methane reforming has been considered individually for their characteristics. From previous researches, the performance of Pt and Rh are exclusively outstanding for the methane reforming. There are several advantages that are benefit to the methane reforming. The features of noble metals are: high activity, which enable reforming process run at lower temperature with high conversion rate; good thermal stability, the noble metal catalyst can remain their activity at high temperature; good selectivity, the conversion rate for desired product is high; high resistance for coke deposition, this character prevent the possibility of coke deposition and protect catalyst from deactivation. The application of noble metals as catalyst for methane reforming attract much attention because of their excellent properties.

However, the high cost of noble catalyst is the main reason why these high effective catalysts cannot be widespread applied in industry scale reformer. Table 2.2 shows the price of metal for catalyst.

From this table, compared to Ni, the price of noble metal is from hundreds time to thousand times higher. Therefore, with higher loadings, Ni has a comparable performance for noble metals such as Pt and Rh, to obtain same quality product. Because of low price, Ni is considered the major catalyst to convert methane into syngas for laboratory scale or industry scale.

Table 2.2 Price of Metal for Catalyst (Source: infomine.com)

Metal	Price(USD/Oz)
Rh	1230.00
Pt	1209.50
Pd	773.50
Ir	540.00
Ru	58.00
Ni	0.4325

2.6.2 Effect of Catalyst Support

The catalyst contains two major parts, active catalytic metal and catalytic support. The duty of the catalytic support is served as a substrate to maintain the active metal stable and high activity under conditions for reforming process. The catalytic support plays a crucial role in the catalytic process. From Table 2.1, different supports with same active metal lead

to various reaction efficient [47]. The reactions of steam methane reforming and CO_2 reforming with methane, which are commonly applied in syngas production, are highly endothermic at temperatures from 700 and 1000°C [67]. Thus, the catalytic support for these reactions must have capability to maintain thermal stability at the high temperature. In this case, the oxides, such as Al_2O_3 and SiO_2, are good options to be used as catalytic support because of their high melting points. Table 2.3 presents the melting points for catalytic support recently studied in reforming reaction [68]. The different oxides such as Al_2O_3, TiO_2, SiO_2, MgO, are commonly used as catalyst supports, which allows larger surface area because of porosity.

2.6.3 Catalyst Preparation

There are two major catalyst preparation technologies applied for industrial catalyst: Precipitation and Impregnation. Precipitation is a process for formation of solid catalyst from liquid solution [69]. The metal salts are dissolved into precipitating reagent using a stirred reactor. And then the filtration, drying, and calcination steps can make catalyst clean to use. The precipitation method can produce catalyst in large amount with uniform property. Another technology for industrial catalyst is impregnation. The solution containing metal salts is dispersed over a high surface area. After removing other solvents by drying, the catalyst is placed in the furnace for calcination to transfer to an active phase. The impregnation process is simpler than precipitation, and the catalyst produced by

impregnation is clearly divided into 2 phase: active phase and support phase. The final activation step for catalyst is the reduction of active metal oxide. The reduction of catalyst is to reach an optimization situation under the limitation of duration period and high activity [70].

In our study, the impregnation method is adopted for convenient. 4.94 g of $Ni(NO_3)_2 \cdot 6H_2O$ is dissolved in 10.0 mL of DI H_2O, and shake the solution until completely dissolved. Then fill a syringe with the $Ni(NO_3)_2 \cdot 6H_2O$ solution, and slowly sprinkle this solution onto 10 g of SiO_2 (or Al_2O_3) pellets in a separate beaker. Rotate and occasionally shake the beaker so as to agitate the SiO_2 (or Al_2O_3) mixture. All of the liquid solution should be absorbed by the silica, if there is any excess present, shake the silica until all the solution is absorbed. Later pour the SiO_2 (or Al_2O_3) on the watch glass in a manner so all the SiO_2 (or Al_2O_3) pellets separate evenly and are exposed to air. The Ni impregnated silica is now green in color. Let the sample air dry overnight after. Preheated the furnace at 300° C and then the resulting brown pellets are calcined in air by placing the entire sample in a muffle furnace at 300° C for 3 h the oven was turned off and allowed to cool to room temperature with the sample in it. Catalyst is taken out from the furnace at room temperature. After preparation, the catalyst is loaded in the fix-bed reactor for upcoming experiment. The catalyst is reduced by H_2 flow at 550° C for 4 h.

2.7 Characterization Methods for Catalyst

Characterization is one of the most important methods to understand the material property of catalyst. By identifying the material property of catalyst, the performance of catalyst, such as activity and level of coke formation, can be analyzed and compared during the reforming process.

2.7.1 X-Ray Diffraction

X-Ray diffraction (XRD) is a non-destructive technique used to characterize crystal structures at the atomic or molecules level and obtain material compositions by analyzed diffraction patterns. Crystal, as diffraction grating, leads to interference effect of light because of coherent scattering. Then, the intensity of scattering incident X-Ray will be enhanced or decreased. In a particular direction, the constructive interference will produce the maximum intensity X-Ray beam, also so know as diffraction X-Ray. This reflection has an angle θ with the surface of crystal. The figure for this reflection is illustrated in Fig. 2.7. When the reflection condition is satisfied, Bragg's law can be applied to calculate the distance between the diffraction planes or incident angle θ.

$$2dsin\theta = n\lambda \qquad (2.8)$$

Where d is the distance between diffraction planes, θ is the X-Ray incident angle, n is an integer, and λ is the wavelength of X-Ray beam. The densities of crystal particles (atoms, ions and molecule) will play a crucial factor on the intensity of reflected X-rays. Since each

crystal structure has individual molecular structural, the XRD pattern is unique for crystal to be identified.

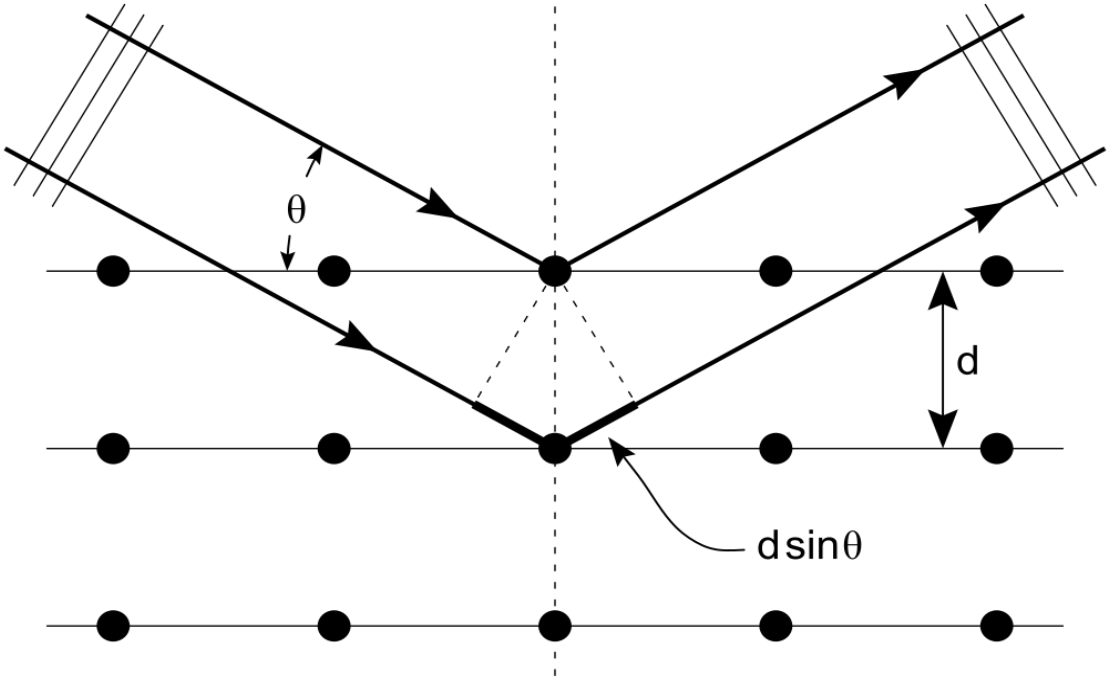

Figure 2.7 Reflection of X-Ray (Source: Wikipedia-XRD)

The XRD pattern is obtained by hitting crystal surface with collimated monochromatic X-Ray beam. The X-Ray source and detector are controlled by computer for automatic rotation based on a pre-setup angle range. This range can be determined either by quick scanning of XRD device or anticipation of material composition. The test sample is grinded into fine homogeneous powder and uniformly pressed into plate. This random distribution of crystal will help clearly identify the reflection.

2.7.2 Scanning Electron Microscope

Scanning electron microscope (SEM) is a precision device used to produces high solution images of catalyst surface in micrometer/nanometer scale. SEM use a very narrow electron beam to scan the catalyst sample and the electron interact with sample for secondary electro emission. Secondary electron can produce a magnified topography image of sample surface by scanning sample point by point. The electron beam is generated and accelerated from an electron gun to an energy in the range 0.1-30 keV (100-30,000 electron volts) [71]. A small electron spot, whose diameter is less than 10 nm, is focused on the surface of specimen to generate signals for image formation. The schematic of SEM is shown in Fig. 2.8. To avoid sharp intensity of current on the surface, samples must be electrically conductive; non-conductive samples are often coated with an ultrathin coating of metal. The vacuum environment is preferred by SEM system to protect electron gun from oxidation and collect more electrons, but technology have been developed that allow imaging biological samples [72].

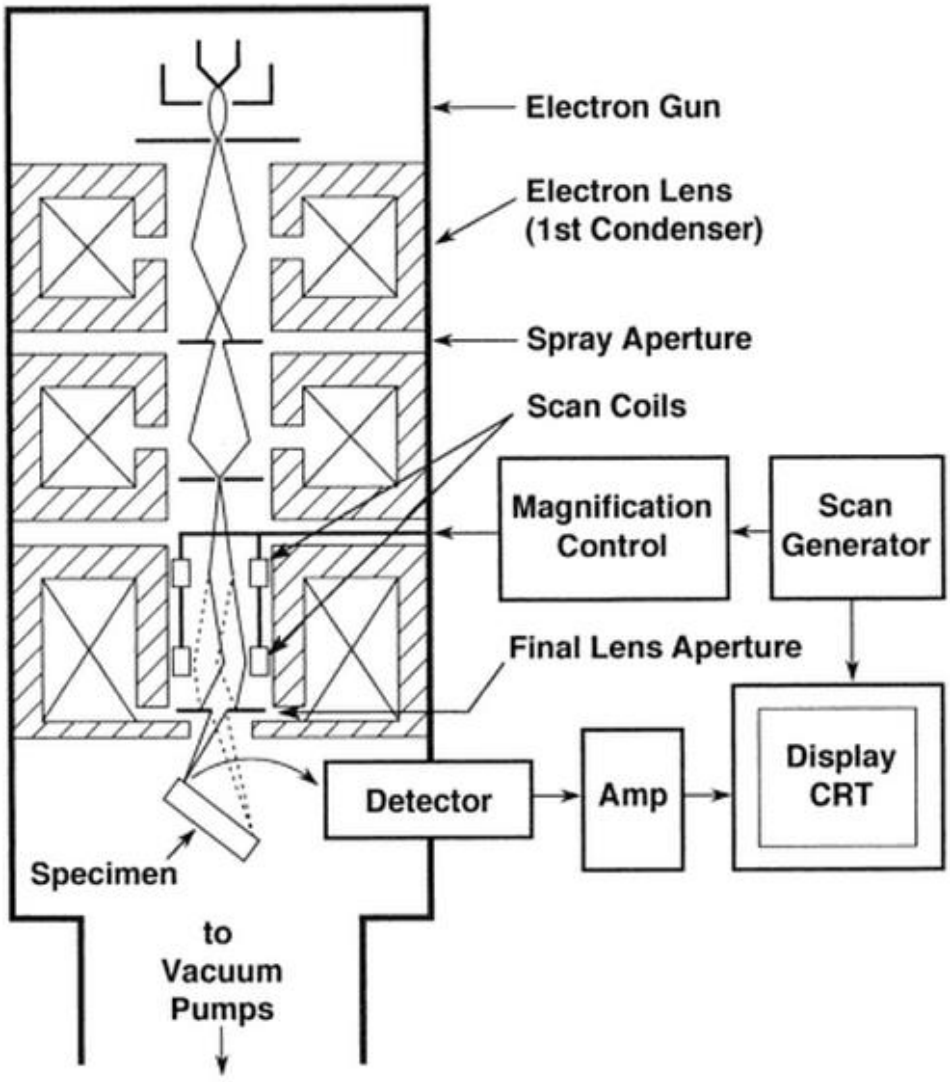

Figure 2.8 Schematic of scanning electron microscope (taken from [73])

Scanning electron microscope manufactured based on the interaction between the electron and the substance. When a high-energy incident electron beam hit surface of the material, the stimulated region will generate secondary electrons, Auger electrons, characteristic X-rays, continuous spectrum X-rays, backscattered electron, transmission electron, as well as electromagnetic radiation in the visible, ultraviolet and infrared light

region. In general, using interaction between electrons and specimen, the physical and chemical property of sample, including morphology, composition, crystal structure and internal electric or magnetic fields, will be obtained. SEM, according to the different mechanism from collected signals, can select research target by using different detector. As for the secondary electrons, the SEM can generate high quality pictures of a sample surface in nanometer scale. Backscattered electron collection is the beam electrons reflected from the sample by elastic or non-elastic scattering. The yield of backscattered electron increases with rise of a sample atomic number, so backscattered electron can not only be used to analyze the morphology, but be used to analyze the ingredients of the sample. Various elements have their own characteristic X-ray wavelength, and the characteristic wavelength depend on the characteristic energy ΔE released during the energy level transition. The collection characteristic X-rays is used to investigate the composition of elements in the sample based on characteristic energy.

2.8 The Gas Chromatography System

Chromatography is a very important analytical technique used to identify and characterize different components in a mixture. The method separates a small gas sample to measure the respective concentrations for each component by different detectors. The sample gas is injected through injection port into the Gas Chromatography (GC) system, and Helium gas as the carrier gas, also known as mobile phase, takes sample into the

column, which contains stationary phase. The sample gas is separated in the column, because the adsorption time for each component to get through stationary phase is different. After separation, the component is sent to a detector by carrier gas to determine concentration for each component. For this study, thermal conductivity detector (TCD) is applied to identify gas component for mixture sample. Since thermal conductivity of the carrier gas (helium) flow is higher than effluent flow from column, the detector will send a signal when capture a temperature rise caused by thermal conductivity drop. The output signal of detector is processed to computer to generate a chromatogram for analysis. The figure 2.9 shows a chromatogram for instance.

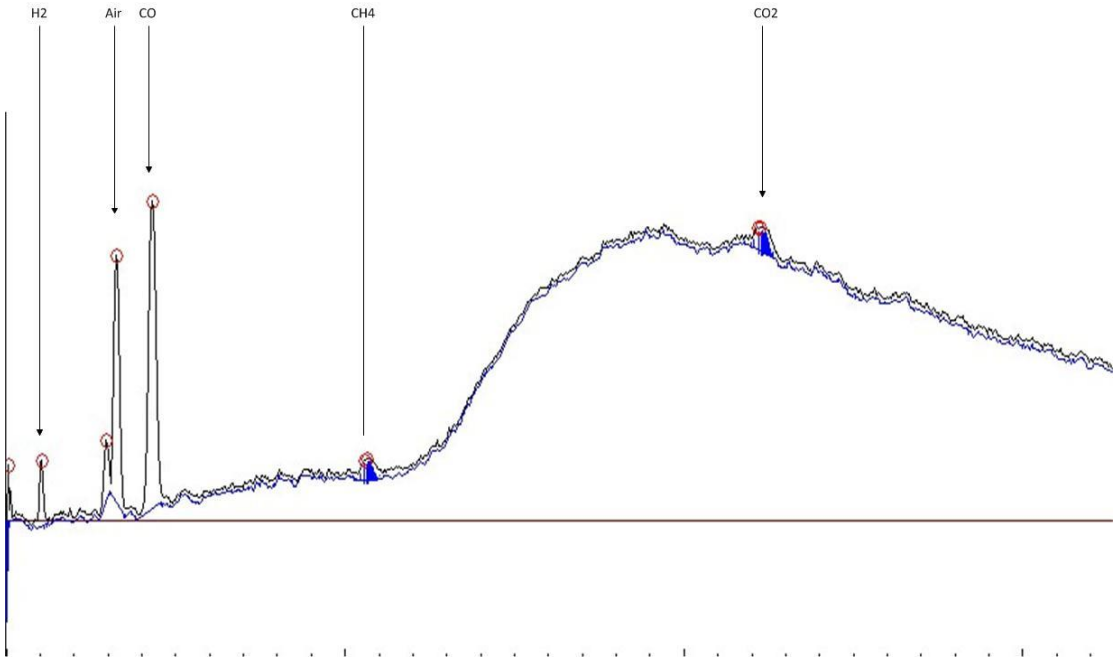

Figure 2.9 Sample Chromatogram (x-time, y-height)

The different peaks represent each constituent, the time related to the specific peak is retention time, and the area of peak has a proportional relation with amount of component. For fixed column conditions, the retention time for specific constituent is repeatable.

SRI model 8610C gas chromatography system is used for product gas composition analysis. This GC system equips a sampling system in heated valve oven, two columns in the heated column oven and a thermal conductivity detector (TCD). The sampling valve contains a 10-port gas sampling valve and a 1mL sample loop. The valve, sample loop and two columns are arranged in a specific order to separate the product gas, including hydrogen, methane, carbon dioxide and carbon monoxide. The operation process of the sampling valve is presented in Figure 2.10. The ten-port sampling valve samples connected with a 1mL sample loop is switch between Load position and Inject position to separate product gas. In the Load position, the product gas flow through the sample loop and carrier gas flow through molecular sieve and silica gel in order. When the valve is switched to the Injection, the sequence of column is reversed with same flow direction. The gas in sample loop is taken to silica gel first by carrier gas, where can capture carbon dioxide and other heavier hydro carbon at 40℃. And then rest of sample gas is sent into the molecular sieve column for component separation. The hydrogen, methane and carbon monoxide flew through the sieve into the TCD to determine the product gas composition. Because of long

retention time for CO_2 in the silica gel column at 40℃, rising oven temperature helps promote rapid elution for silica gel column.

The data system of GC and PeakSimple software is used for control the process and data acquisition. The working temperature of GC and status of sampling valve is programmed by PeakSimple software. The sample gas is obtained every half hour, which allow all components of product gas to be completely separated and recognized by detector.

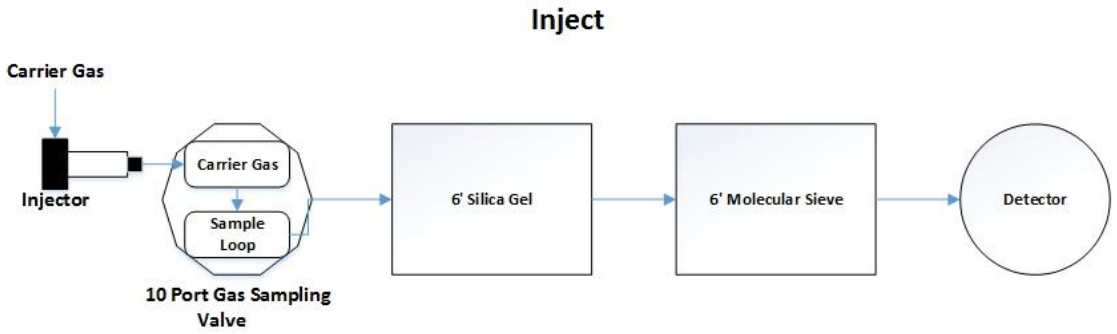

(a)

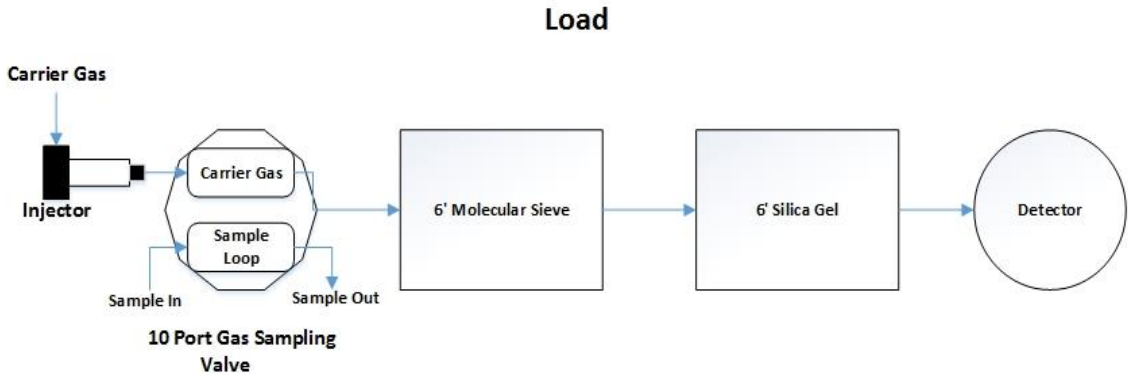

(b)

Figure 2.10 Operation Process of 10-Port Gas Sampling Valve

(a) Inject Position (Relay G: On); (b) Load Position (Relay G: Off)

The calibration of GC system is a very important step for calculating gas composition by providing a standard. Standard gas, including pure gas and mixture gas, is used to calibrate GC. Because the main product for this research includes hydrogen, methane, carbon dioxide and carbon monoxide, calibration points for each pure gas are recorded by generating single gas chromatogram with difference volumes. And mixture gas, whose composition is known, flow through GC to verify calibration results. The formulas, which relates the mass and area, and curves of calibration for single gas are shown in figures from 2.11 to 2.14.

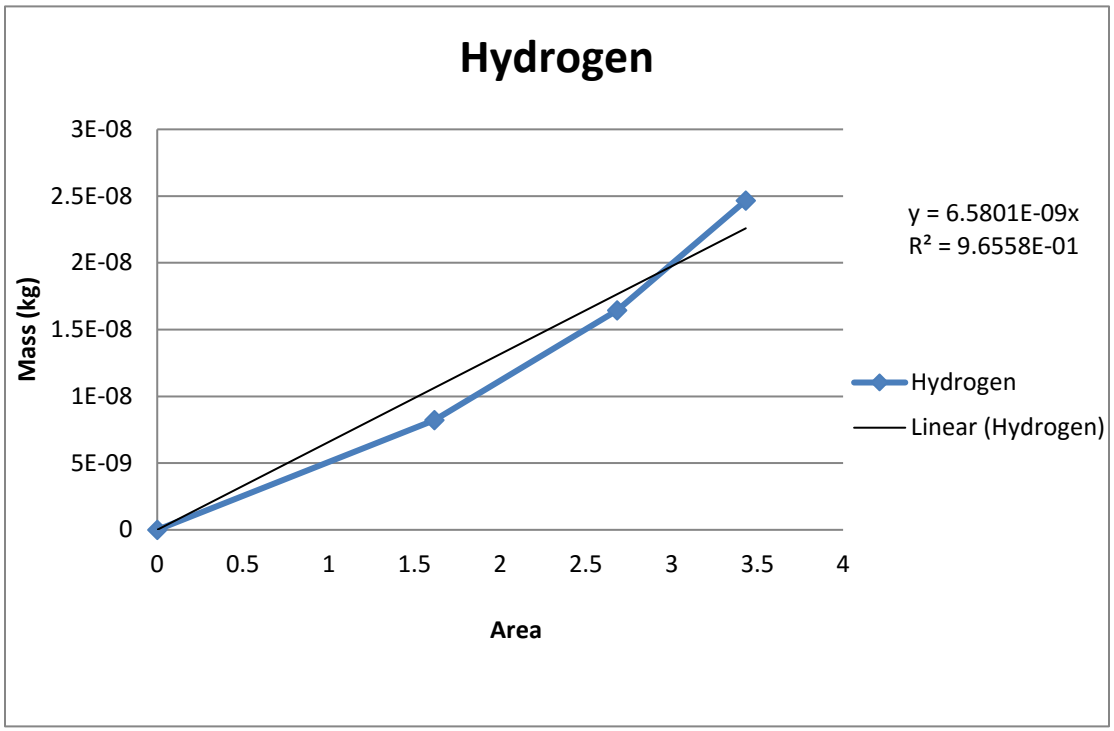

Figure 2.11 GC Calibration Curves of Hydrogen

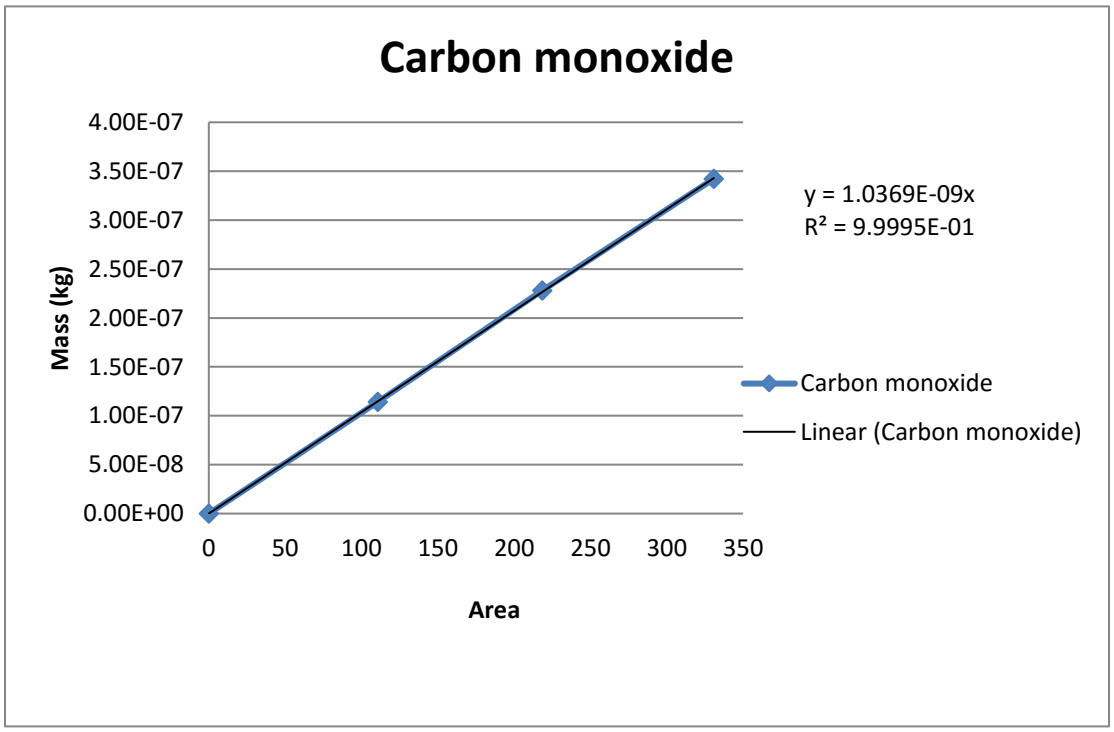

Figure 2.12 GC Calibration Curves of Carbon Monoxide

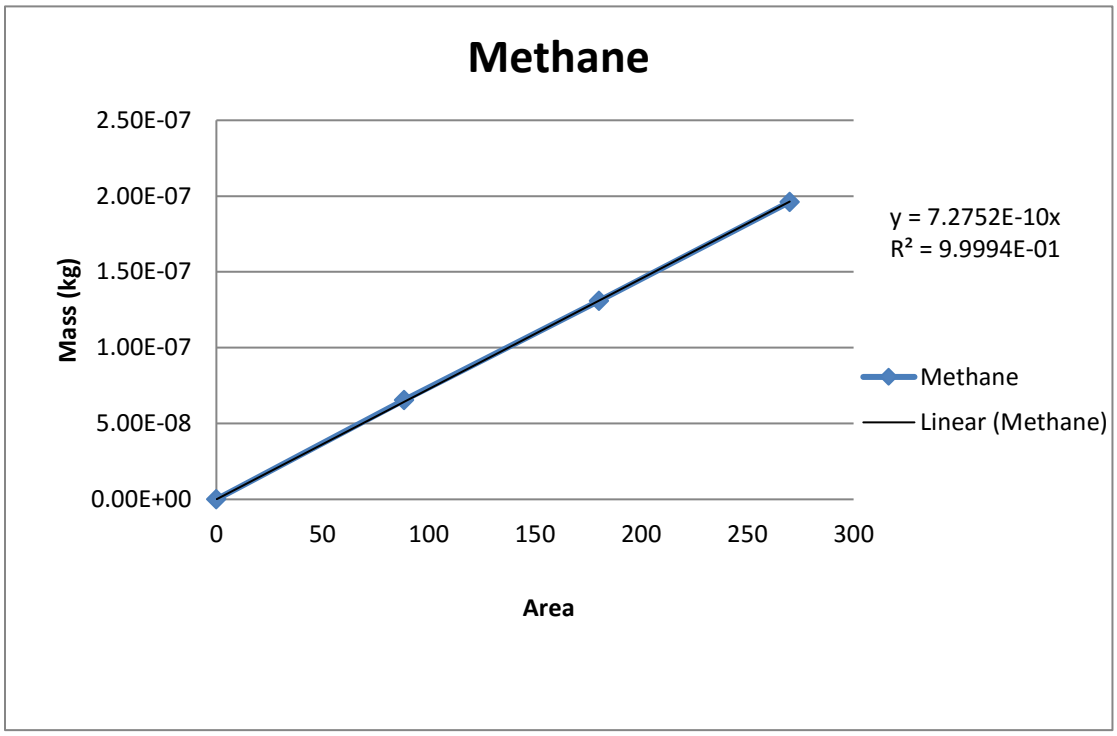

Figure 2.13 GC Calibration Curves of Hydrogen

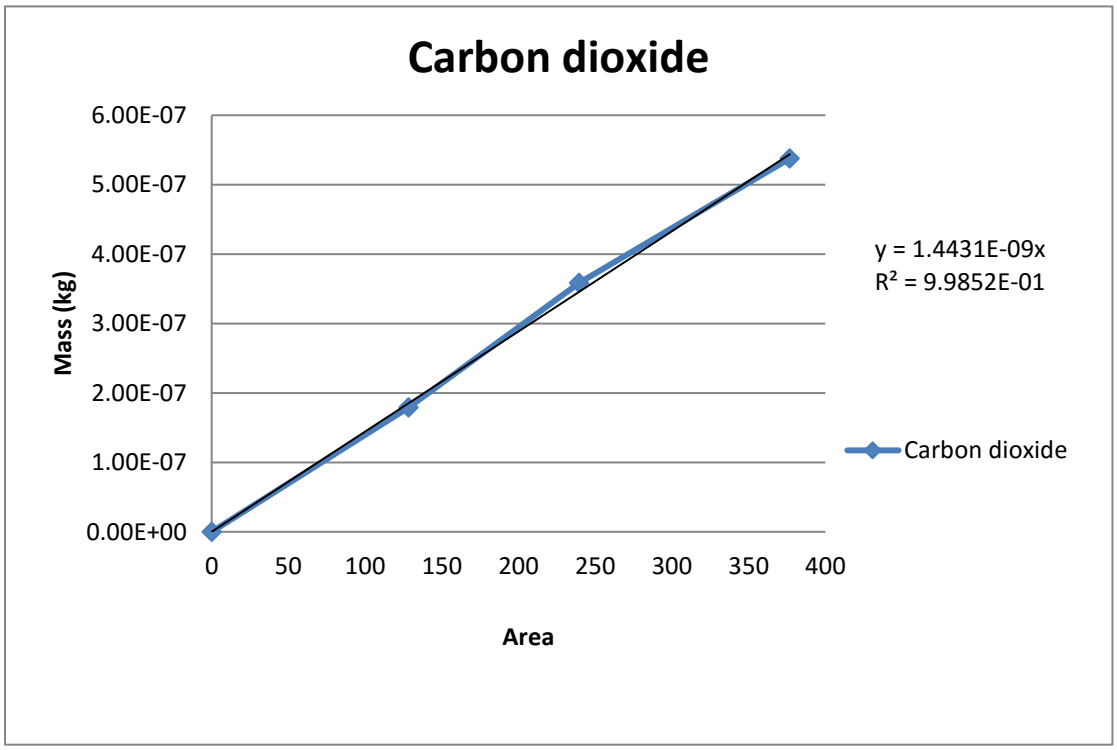

Figure 2.14 GC Calibration Curves of Carbon Dioxide

2.9 Flow Control and Measurement

The measure and control of gas flow is essential for experiment results. The product gas from chemical reaction is highly related to the amount of reactant. There are three devices applied in this research, including NE-500 micro pump, KI 60410-R3 flow meter and Omega FMA 5400 series mass flow controller.

The NE-500 syringe micro pump is used to push water into the steam generator, and then send steam into the reactor mixing with methane for the steam reforming. The pump is programmable and connected to computer with RS-232 communication port, which could offer precise and continuous water flow as reactant. A BD syringe (30ml with ID 21.59mm) was fixed on the micro pump with flow range from 15.4 μL/Hr to 1120 mL/Hr. The tip of syringe is connected to steam generator using Teflon and steel tube.

KI 60410-R3 flow meter and Omega FMA 5400 series mass flow controller is applied to monitor and control the gas flow rate. The vertical installed KI60410-R3 flow meter is a conventional flowmeter with a glass tube, which contains a black glass float with 1/8 inch diameter. An adjustable valve provides gas (air) flow range from 21.7 to 905 CCM. Compared to conventional flow meter, the Omega FMA 5400 series features a built-in electromagnetic valve for maintaining a continuous flow rate without affection from parameter variations. And a digit display is more precise and convenient for viewing and

recording. Meanwhile, this device also provides a wide flow range from 10 SCCM to 1000 SLM.

For both of two types flow meter, the direct reading from device is based on a reference gas (Nitrogen). Therefore, the calibration conversions from reference gas is required. The K factor is adopted in calibration conversion, which is derived from gas density and coefficient of specific heat. The relationship is shown in equation 2.9.

$$K_{gas} = \frac{1}{d \times C_p} \qquad (2.9)$$

Where, d = gas density (gram/liter)

C_p = coefficient of specific heat (Cal/gram)

The relative K factor is used to converse mass flow rate of the reference gas to actual gas.

$$K = \frac{Q_a}{Q_r} = \frac{K_a}{K_r} \qquad (2.10)$$

Where, Q_a = mass flow rate of an actual gas (SCCM)

Q_r = mass flow rate of a reference gas (SCCM)

K_a = K factor of an actual gas

K_r = K factor of a reference gas

Table 2.3 Gas Factor Table

Actual Gas	K Factor relative to N_2	C_p (Cal/g)	Density (g/L)
Air	1.0000	0.240	1.293
Nitrogen N_2	1.0000	0.2485	1.25
Carbon Dioxide CO_2	0.7382	0.2016	1.964
Methane CH_4	0.7175	0.5328	0.715

Chapter 3
STEAM REFORMING EXPERIMENTS
(CH_4-H_2O REFORMING)

Steam reforming technology is most broadly applied in industry to produce syngas. In this study, this technology is applied as a feasible method to supply feedstock syngas for Fischer-Tropsch synthesis. The experiment system for steam reforming is mainly combined with two parts, reactor and steam generator. This chapter will discuss the concept of reactor design, material, the experimental setup and procedure. In the last part of this chapter, the experimental results will be described.

3.1 Reactor Concept

The fixed bed reactor is used in this research, because this type of reactor is able to supply a continusous and reliable flow. And the simple structure of reactor can be easily setup in laboratory with low cost. A stainless steel tube is chosen as the reactor with inner diameter 1/8 inch because of high temperature. The design of the reactor is presented in Figure 3.1. The single reactor is horizontaly placed in the experimental system to make the catalyst dispersed constantly in the desired location. The reactor contains 1.5 inch SiO_2 pellets (or Steel Wool), 10 inch Ni catalyst, and another 2.5 inch SiO_2 pellets (or Steel Wool). Two SiO_2 (or Steel Wool) zones keep catalyst fixed at a precise length.

The reactor is cleaned using water and acetone before catalyst loading. First, the thermocouple is connected to outlet of the reactor with a T-shape conector, and tip of thermal couple is approximately in the middle of catalyst bed. Some SiO_2 pellets (or Steel Wool) are loaded and pushed to bottom of the reactor. The amount of catalyst particles is measured and filled into reactor, and then gently knock and shake the reactor tube to pack the constantly catalyst at the exact volume. Another SiO_2 pellets (or Steel Wool) are filled in the inlet of reactor to fix catalyst.

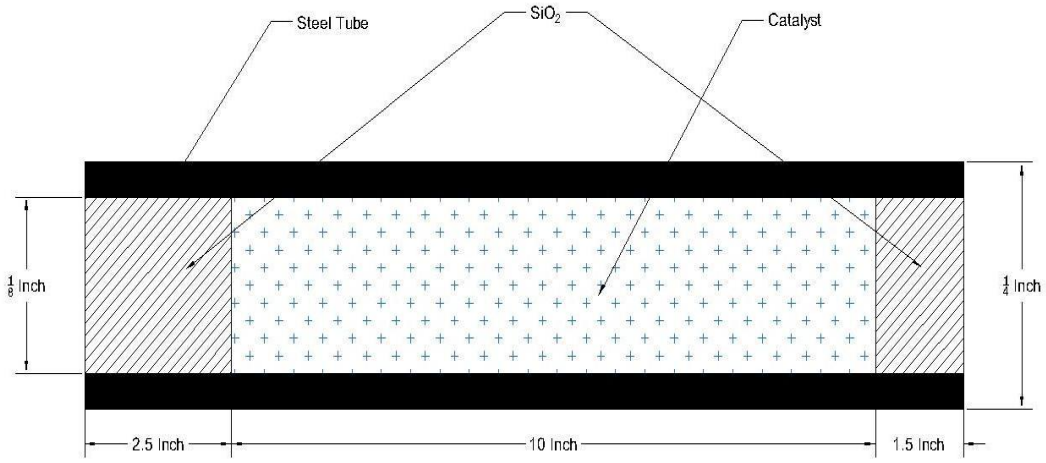

Figure 3.1 Design of Reactor

3.2 Materials

3.2.1 Feed Gases

The natural gas is the most common feedstock in the syngas production. Therefore, as the major part of natural gas, methane is the main feedstock in this research combined with steam for reforming experiment. The hydrogen is used for preliminary test to reduce catalyst. The helium is inert carrier gas in the gas chromatography system. Because the catalyst is very sensitive for carbon deposition and poison. The gas involved in this study has a high-purity grade.

3.2.2 Catalyst Support

As discussed in Chapter 2.6.2, the catalyst support plays an important role in maintain activity of catalyst. The SiO_2 is mainly used as support in this study to enhance the catalytic activity because of physical and chemical properties. The high melting point and mechanical strength of SiO_2 can avoid catalyst deactivation form phase transition or crystal transformation at a high reaction temperature. The properties of commercial SiO_2 is listed in Table 3.1.

Table 3.1 Properties of SiO_2

Material	SiO_2
Size and Shape	3 mm Pellets
Surface Area, m^2/g	274
Crush Strength, lbs	9.1
Packing Density, lbs/W	25.2
Total Pore Volume, Hg, cc/g	1.12
Median Pore Diameter, Angstroms	114

3.2.3 Catalyst

For reforming reaction, various transition and noble metals are used as main component of catalyst. In chapter 2.6.1, it mentioned that noble metals are more effective and stable as catalyst in the reforming process compared to non-precious metals. However, the high price of precious metals is the major drawback for using in industry scale reforming. Ni with low cost and wide availability, which is able to substitute noble metals as catalyst, has been extensively studied [73]. In this experimental study, Ni is applied as the catalyst for reforming reaction. The Ni catalyst is produced by an impregnation method, and the schematic of the impregnation process is presented in Figure 3.2. The solution of Ni salt is uniformly dispersed over support particles. After drying and calcination, the fresh catalyst is ready to load into the reactor. The catalyst produced by this method can avoid carbon deposition while reduced active sites for carbon formation [36].

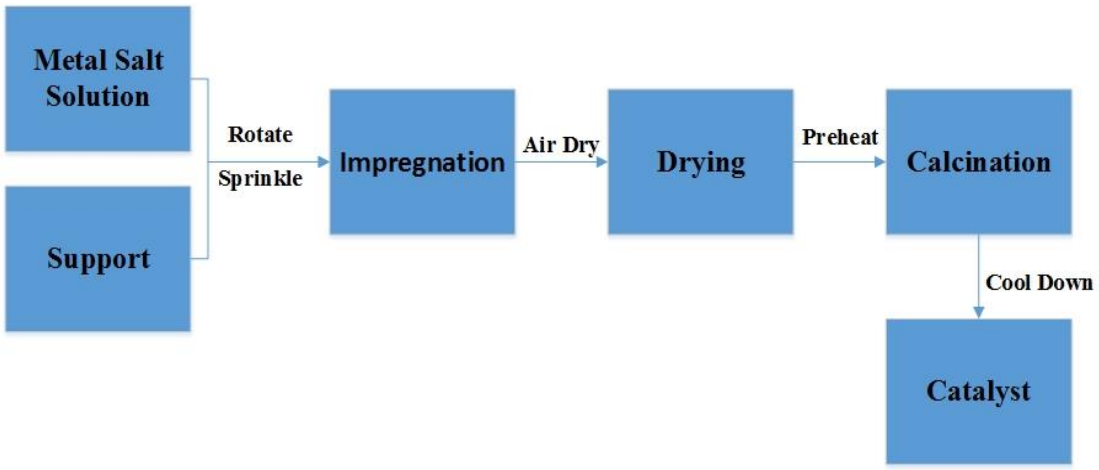

Figure 3.2 Schematic of Catalyst Preparation

3.3 Experimental Setup

Figure 3.3 shows the schematic diagram of experimental system applied in the reforming process. The two gas cylinders contains high purity hydrogen for catalyst reduction and methane as feedstock. The gas flow rate and pressure is controlled by a high pressure regulator on the gas cylinder. A flow meter (KI instrument Model 60410-R3) was installed to regulate the flow rates of the inlet gas, hydrogen and methane. The flow is pre-calibrated by manufacture with standard gas and converse calibration to feed gas by user for this experiment. A check valve is placed between gas cylinder and flow meter to prevent back flow from reactor caused by pressure drop during reaction. The water is pushed into steam generator by a NE-500 syringe micro pump, the flow rate is programmed from PC termination. The liquid water is evaporated in the steam generator, and high temperature steam is fed into reactor mixed with feed gas. The steam generator, reactor and connection

tube are insulated to keep the high temperature, which retain water in gas phase during reforming reaction.

The feed gas containing methane and pre-heated water steam flow into tube reactor horizontally. The feed gas is heated up to designated temperature and flow through catalyst bed in the tube reactor. After exiting from outlet of reactor, the product gas flow through a conventional flask condenser with water bed to remove excess steam for sample collection. The product gas is collected into a customized sample bag made by FlexFoil from SKC Inc., which could help trap H_2 inside for as long as three days. Then, a small amount is extracted by using microliter syringe and sent to a gas chromatography (GC) system for analysis.

The reactor was designed and setup for this methane steam reforming experiment. The concept of reactor is to product feedstock for Fischer-Tropsch synthesis process in a lab scale. Therefore, a simple and reliable type of reactor, the fixed-bed reactor, is chosen for experiment. The reactor is made of stainless steel tube with a 1/4-inch OD (outer diameter) and a 1/8-inch ID (inner diameter). The capacity of the reactor is able to keep up to 5g catalyst inside and has ability to support reaction at the high temperature.

The ceramic heating coil wire is uniformly wrapped on the reactor and steam generator to maintain temperature constant in the reactor and keep water steam away from condensing. The reactor temperature is controlled and maintained by an Omega PID (proportional-integral-derivative) controller system. The system has three parts: the

temperature controller, the relay and the thermal couple. This temperature control system can precisely regulate the reactor temperature through a PID control strategy. The heating rate is governed by this system to avoid any sharp temperature rising, which may destruct the catalyst. A variac transformer is used as power supply for ceramic heating wire. This device is also connected with temperature control system to control power output. The Figure 3.4 is a picture for setting up of the methane reforming experiment.

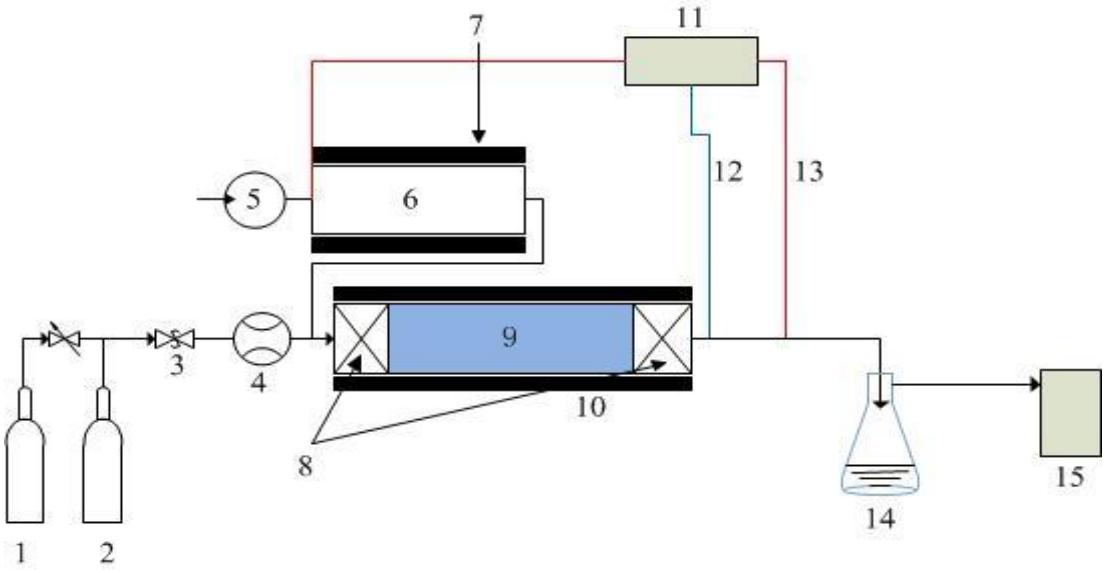

Figure 3.3 Schematic Diagram of Methane Reformer

1. H2 Tank 2. CH4 Tank 3. Safety Valve 4. Flow Meter 5. Programmable Syringe Pump 6. Steam Evaporator 7. Ceramic Insulator 8. SiO_2 9. Catalyst Bed 10. Reactor 11. Temperature Controller 12. Thermal Couple 13. Ceramic Heating Wire 14. Collector 15. Sample Gas Bag

Figure 3.4 Experiment Setup of Methane Reformer

3.4 Experimental Procedure

The feed gas including methane and steam is fed into reactor from two different lines. For each gas line, the flow rate is controlled and monitored. The reforming reaction is carried out at atmosphere pressure in stainless steel tube reactor. A type-K thermal couple from PID control system is insert from outlet of reactor to monitor the temperature at the catalyst bed.

After catalyst loading, the first step before experiment is to reduce the catalyst for activation under hydrogen flow. The catalyst bed is heat up to 550° C for 4 hours with a 50 sccm hydrogen flow. The residual reducing gas is flushed out by a methane flow to provide a steady state before experiment conduct. Before start pumping water into the

steam generator, the line temperature is preheated to a temperature above 200° C to remove potential condensed water in the reactor. Then the mixture gas of H_2O and CH_4 at a specific ratio is reacted in the reactor at a designated temperature. The reactor temperature is controlled by a PID controller and raised slowly, that the heating rate is around 10℃/min, from room temperature to reacting temperature for 2 hours. Then the experiment temperature is maintained for 4-6 hours for sampling. The effluent gas from the reactor is sent into the condenser to clean product gas for sampling. The expectation of product gas includes methane, hydrogen, carbon monoxide and carbon dioxide. Because of extremely toxic CO, the collection step is limited in the experimental hood with ventilation system. And the rest of product gas is also need to be processed to exhaust system. Gas Chromatograph (GC) is used for analyzing product composition by measuring area peaks for each single component. The SRI Model 8610C Gas Chromatograph system is controlled by Peak Simple software to identify peak area value, generate chromatogram, and process data. The experiment data is evaluated by calculation for methane conversion rate from reactant gas composition and product gas composition. When the experiment is finish, the water line is shut off first to avoid water accumulation in the reactor. Then the methane flow is maintained until the temperature decreases to a low level.

3.5 Experimental Data Process

The steam methane reforming process is mainly consisted for three reversible reactions.

$CH_4 + H_2O \leftrightarrow CO + 3H_2$ (3.1)

$CO + H_2O \leftrightarrow CO_2 + H_2$ (3.2)

$CH_4 + 2H_2O \leftrightarrow CO_2 + 4H_2$ (3.3)

The Equation 3.3 is combined from main reaction (Eq.3.1) and water gas shift reaction (Eq.3.2). The calculations for conversion rate of reactant gas and yield of product gas are presented in Equation 3.4 to 3.7.

Methane conversion: $X_{CH_4} = \frac{[CH_4]_{(in)} - [CH_4]_{(out)}}{[CH_4]_{(in)}} \times 100\%$ (3.4)

Hydrogen yield: $Y_{H_2} = \frac{[H_2]_{(out)}}{3 * ([CH_4]_{(in)} - [CH_4]_{(out)})} \times 100\%$ (3.5)

Carbon monoxide yield: $Y_{CO} = \frac{[CO]_{(out)}}{[CH_4]_{(in)} - [CH_4]_{(out)}} \times 100\%$ (3.6)

Carbon dioxide selectivity: $S_{CO_2} = \frac{[CO_2]_{(out)}}{[CO]_{(out)} + [CO_2]_{(out)}} \times 100\%$ (3.7)

Where X, S, and Y are conversion, selectivity and yield, respectively.

3.6 Experimental Results

The performance of experiment is mainly effected by two major parameters, temperature and Steam/Carbon (S/C) Ratio. In this experiment, the temperature range is set from 700℃ to 800℃. And the S/C ratio is set from 1 to 4.

3.6.1 Effect of Temperature

Since the Methane Steam Reforming reaction is highly endothermic, increasing the temperature is favored to reaction rate. In these runs, the pressure in the reactor is set at 1 atm. Figure 3.5 shows the effect of temperature on reaction performance, the Steam/Methane ratio for reactant gas is 3 and the residence time is 8.78 s. As illustrated, CH_4 conversion rate rises with the increase of temperature. The highest conversions rate 97.6% is obtained at the temperature of 800℃. Meanwhile, temperature is also a significant factor for product gas composition. Figure 3.6 indicates that H_2/CO ratio of product gas decreased alongside increasing reaction temperature. From this figure, the H_2/CO ratio is higher than the theoretic value for steam reforming reaction and lower than combine reaction, which indicates that water gas shift reaction is involved in the experiment during the process. Because the WGS reaction is exothermic process, this process is depressed at higher temperature. Less CO is involved in reaction to product CO_2 with steam. From figure 3.7, CO_2 selectivity drops as the effect of the WGS reaction has been weakened at

high temperatures. Therefore, H_2/CO ratio decreased at higher temperatures, at which the WGS reaction is restricted during the methane reforming process.

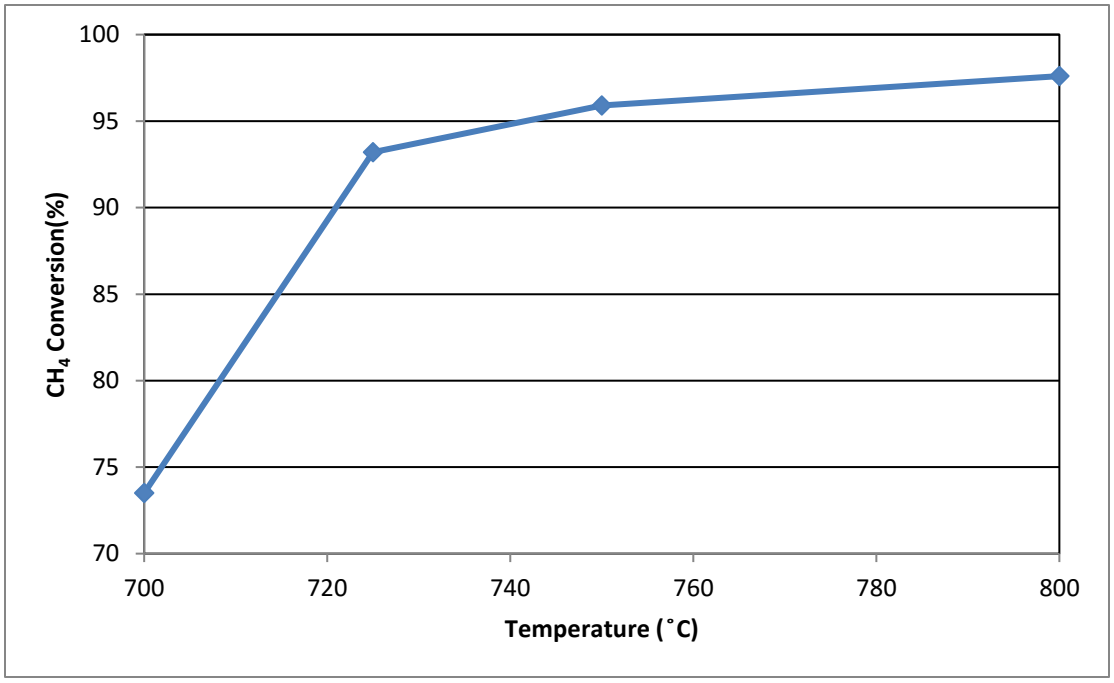

Figure 3.5 CH_4 conversion as a function of Temperature for SMR

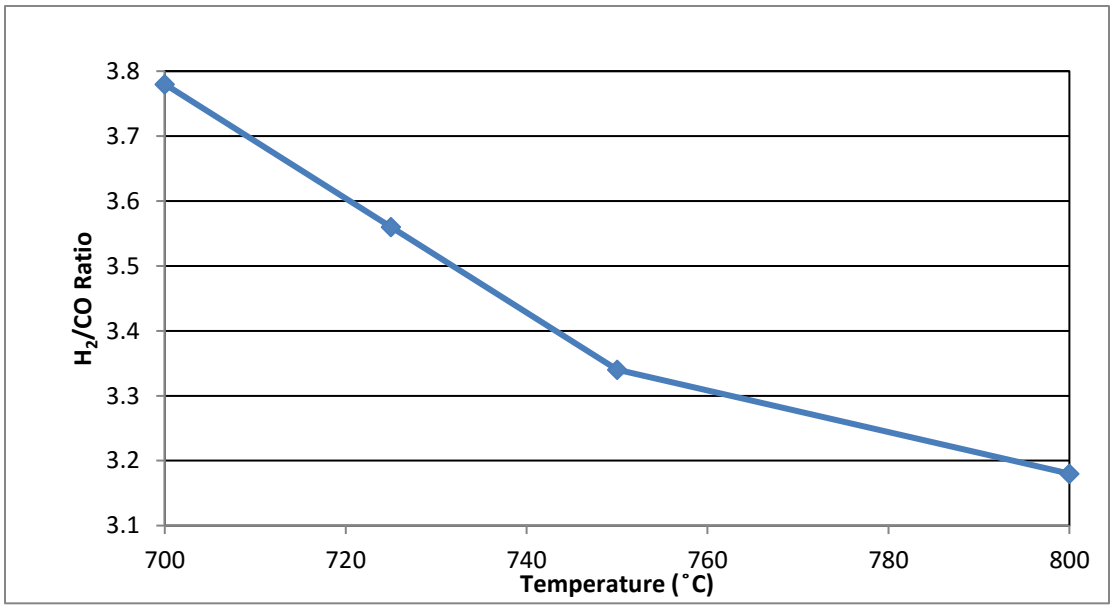

Figure 3.6 H_2/CO Ratio as a function of Temperature for SMR

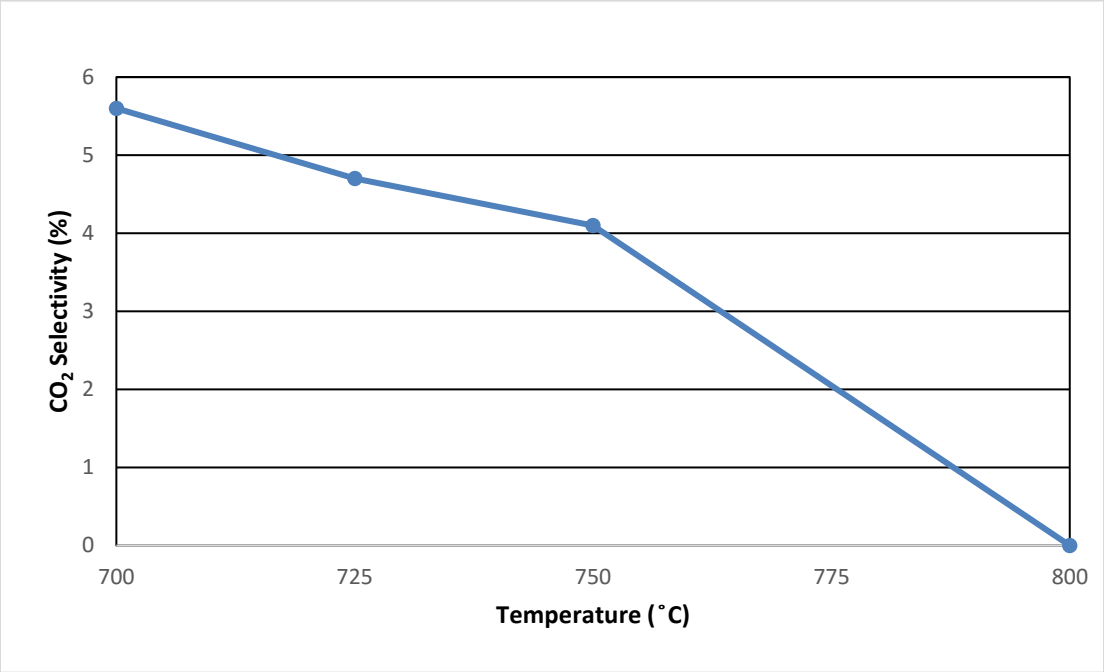

Figure 3.7 CO_2 selectivity as a function of Temperature for SMR

3.6.2 Effect of S/C (Steam/Carbon) Ratio

Steam to Carbon (S/C) ratio or Steam Methane ratio is another major parameter to effect steam reforming. From the steam reforming reaction and combined reaction with WGS, the theoretic S/C ratio is 1 and 2. The higher S/C ratio is usually applied to prevent carbon deposition by oxidizing carbon in Equation 3.8.

$$C + H_2O \longleftrightarrow CO + H_2 \qquad (3.8)$$

The S/C ratio has attracted a lot of attention, and numbers of studies about the effect of S/C ratio in steam reforming reaction have been performed. [74][75][76] Based on stoichiometric ratio of reaction and previous research result, the S/C ratio is set from 1 to 4 for this experiment. Figure 3.8 shows the effect of S/C ratio on the reactor performance,

the residence time in the reactor is 8.78s and the temperature is set at 800℃. Although the methane conversion rate maintains at a high level from S/C ratio from 1 to 4, the conversion rate at S/C ratio 3 is higher than others. Figure 3.9 shows the effect of S/C ratio on the H_2/CO ratio at 800℃, which would be the optimized operating temperature for the Steam Methane Reforming reaction in reactors. It states that H_2/CO Ratio increased with rising S/C Ratio. As mentioned in the last section, the WGS reaction did not contribute to the products. The excess amount of steam is adopted by WGS, therefore the H_2 composition of product gas is increased. Also from Figure 3.10, the CO_2 is sharply increase to 19.74% at S/C ratio 4, which also prove the WGS process effect the product gas for steam reforming. The purpose for this study is to supply feedstock for F-T process. Therefore, a specific H_2/CO ratio is required with proper S/C ratio selection.

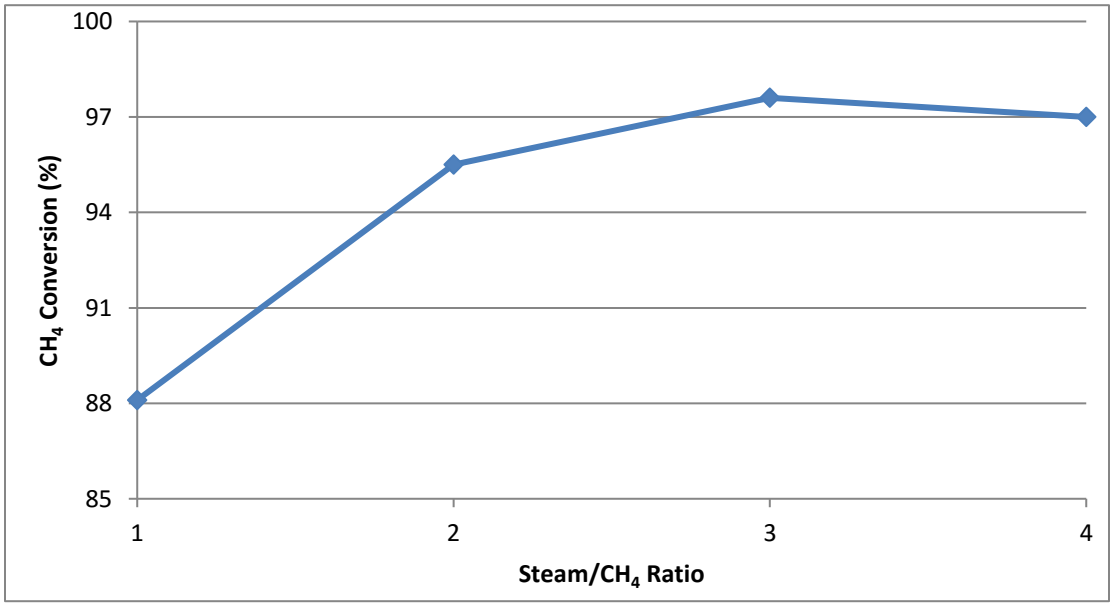

Figure 3.8 CH_4 Conversion as a function of S/C Ratio

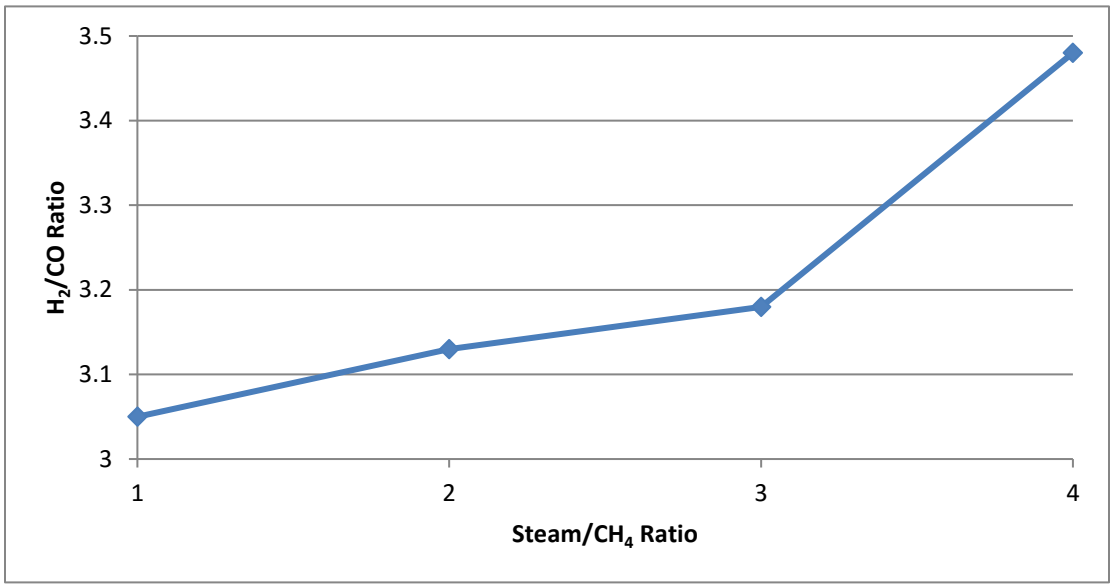

Figure 3.9 H_2/CO Ratio as a function of S/C Ratio

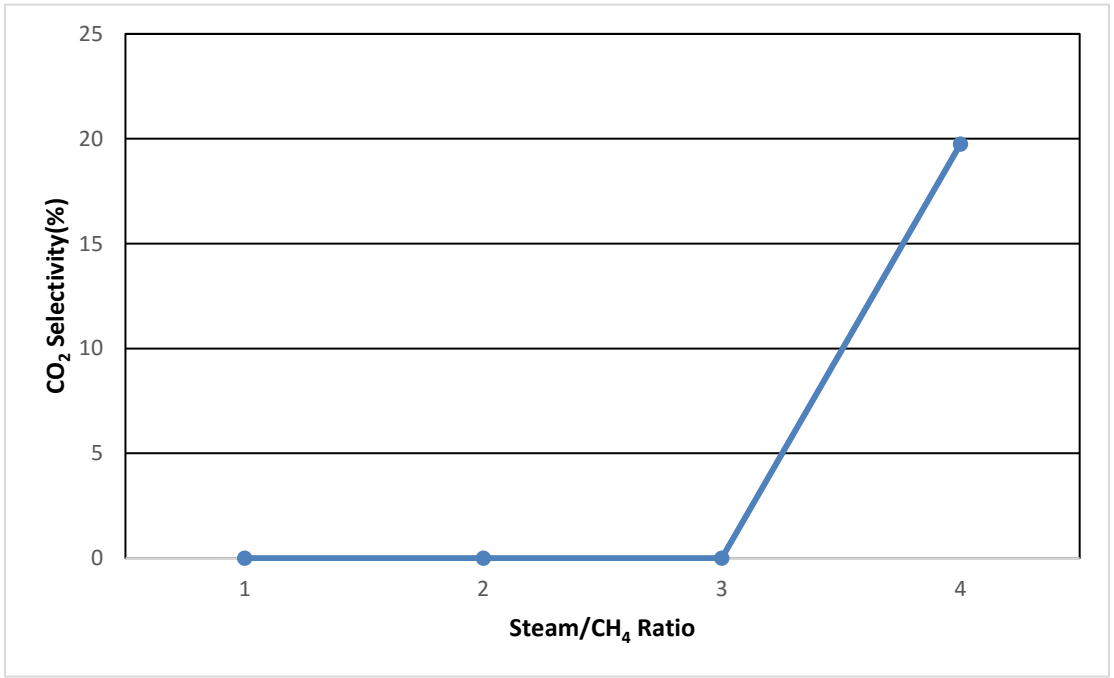

Figure 3.10 CO_2 selectivity as a function of S/C Ratio

3.7 Catalyst Analysis

Carbon deposition is the major problem in the process of methane steam reforming. The coke covers the active site of catalyst to cause deactivation and the coke particle accumulate inside reactor to block reactor tube. To protect the reactor, the catalyst is renewed every 2 weeks for up to 80 hours. For further improvement for the research, the catalyst after reaction is examined by XRD and EDAX spectrum to characterize carbon formation. The Figure 3.11 shows the XRD pattern of Ni/SiO_2 Catalyst after reforming reaction. The diffraction peak around 20˚ represents carbon component appeared in the catalyst. From spectrum results in Figure 3.11, the weight of carbon component is over 15% for the catalyst. Therefore, although the Ni/SiO_2 Catalyst is able to maintain activity for long period running, the formation of carbon eventually cause deactivation. The operation conditions for the experiment system should be optimized to maximize the catalyst working life.

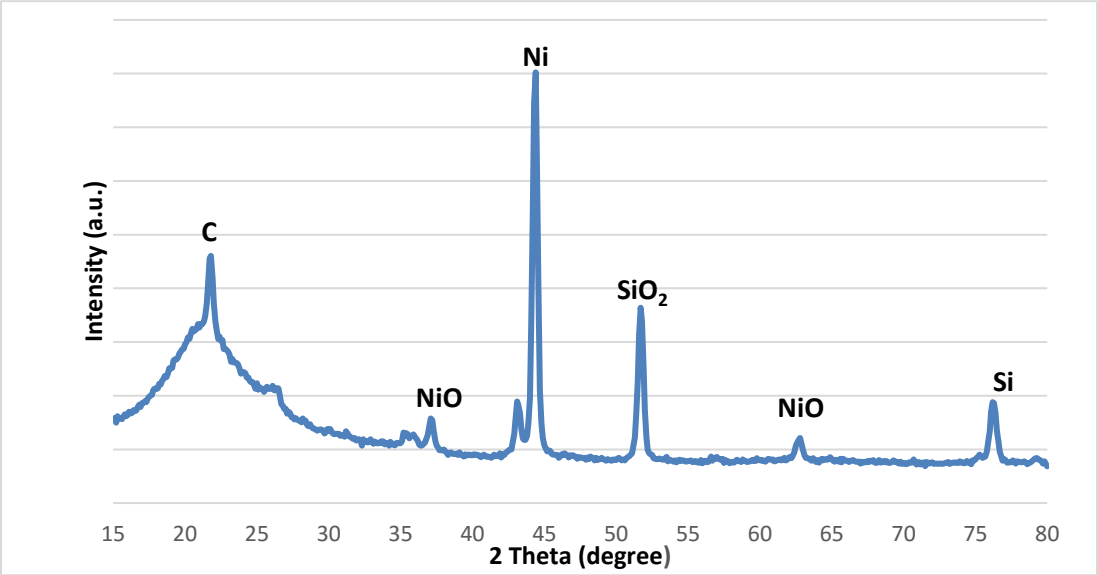

Figure 3.11 XRD pattern of Ni/SiO_2 after reaction

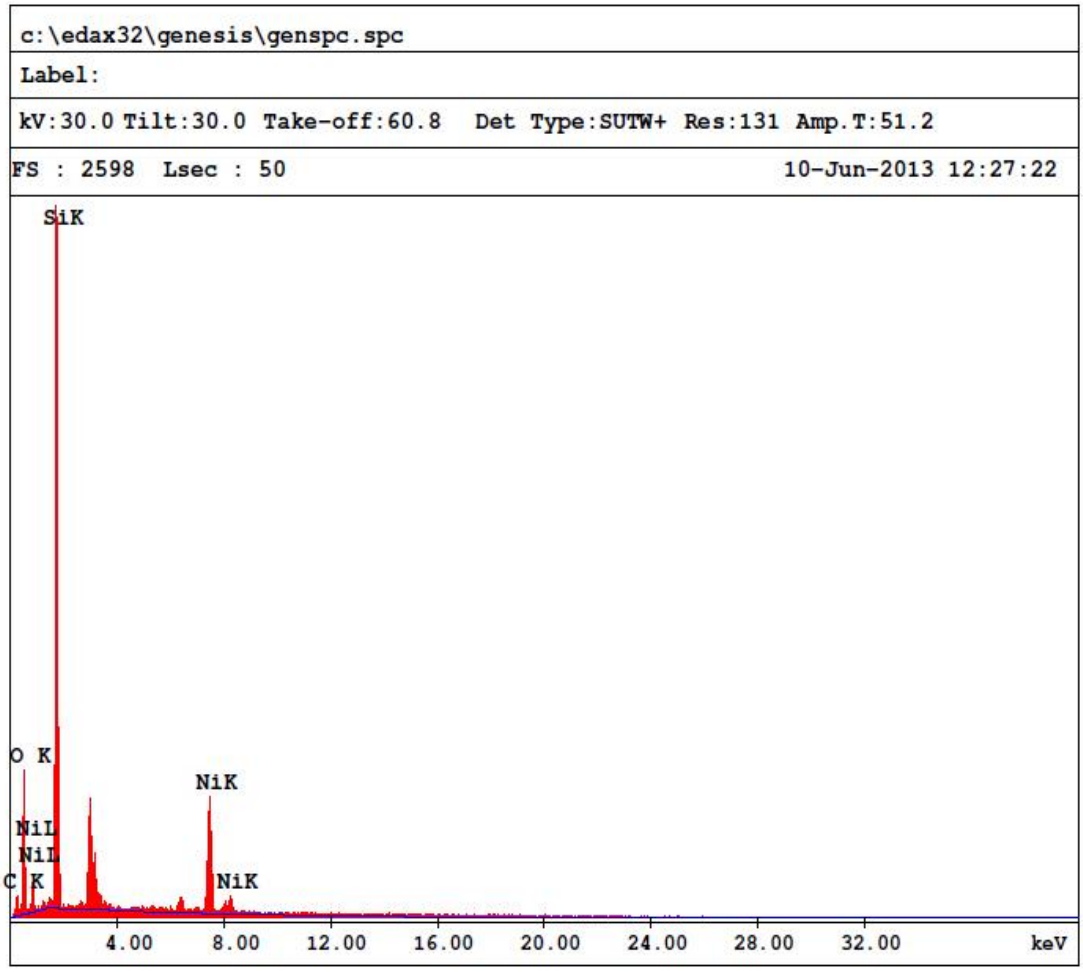

EDAX ZAF Quantification (Standardless)
Element Normalized
SEC Table : Default

Element	Wt %	At %	K-Ratio	Z	A	F
C K	16.45	30.00	0.0215	1.0486	0.1249	1.0003
O K	23.76	32.52	0.0583	1.0338	0.2371	1.0011
SiK	37.31	29.10	0.2401	0.9974	0.6452	1.0000
NiK	22.48	8.39	0.2063	0.9131	1.0053	1.0000
Total	100.00	100.00				

Element	Net Inte.	Bkgd Inte.	Inte. Error	P/B
C K	7.64	0.66	5.54	11.58
O K	58.92	1.46	1.89	40.36
SiK	377.96	6.38	0.74	59.24
NiK	100.82	4.46	1.47	22.61

Figure 3.11 EDAX Spectrum Results of Ni/SiO_2 after reaction

3.8 Summary

In this chapter, the experiment system for steam methane reforming has been discussed. This study states the mechanism of methane reforming for syngas production and application in the Fischer-Tropsch Process. A reformer reactor was built to be analyzed the performance and product gas composition. The catalytic performance of Ni is also characterized. As catalyst support, SiO_2 helped form active catalyst site and secure under experiment conditions. Using the fixed-bed continuous reactor at high temperature, Ni exhibits excellent performance in the Steam Methane Reforming with S/C ratio 3, since the CH_4 conversion reached above 90%. Although carbon deposition was detected from XRD and spectrum analysis, reaction process was able to last for over 60h running with different S/C Ratios. The results of temperature and S/C Ratio characterizations also demonstrated that this type of methane reformer would be promising and practical for the production of syngas. The modification for reactor and future work will be discussed in the last chapter.

Chapter 4
DRY REFORMING EXPERIMENTS
(CH_4-CO_2 REFORMING)

In this chapter, the experiment system is built up based on CH_4-CO_2 reforming reaction. Compared to the conventional steam reforming experiment system, the design is simplified by removing the steam generator and water pump. This chapter will present the experimental setup and procedure, especially focusing on modifications from previous study. Meanwhile, the effect of temperature is also involved to evaluate the reactor performance. This experiment also includes characterization of Ni/SiO_2 catalyst for CO_2 reforming, and a durability test for catalyst is discussed.

4.1 Introduction

The product gas from CO_2 reforming has a lower H_2/CO ratio than steam reforming, which is another promising method to product feedstock for the F-T process. Moreover, the consumption of two major greenhouse gases during reaction show great potential for enviroment protection. However, the concentration of carbon element is higher than steam reforming which leads to rapid carbon formation. The Ni catalyst suffers deactivation from carbon deposition, which also plugs the reactor to cause reaction failure. Therefore, besides the conversion rate for feed gas and composition of product gas, how to protect the catalyst from carbon deposition is also an important study area for this research. This chapter

includes three major parts. First, the effect of temperature is discussed to evaluate process effiency. The reactor for dry reforming is a fixed bed type reactor the same as steam reforming reaction because of its reliable performance and low cost. The temperature range is set from 500° C to 700° C. Second, the catalyst is chacterized to analyze carbon deposition in the reaction. Third, a 24 hour non-stop test is conducted to prove catalyst duralbility in a high temperature, high carbon enviroment.

4.2 Materials

The Feed gas for this experiment contains methane and carbon dioxide with high purity. And high purity grade hydrogen and helium are applied as service gas for catalyst reduction and inert carrier gas of the GC system, respectively. All other experiment information for catalyst, properties of support and catalyst preparation is mentioned in Section 3.2.2 and 3.2.3 from Chapter 3. The Ni/SiO_2 is used for the dry reforming reaction, and the catalytic performance is investigated.

4.3 Experimental Setup

The setup of CO_2 reforming experiment platform is similar to previous steam reforming experiment. The design of the reactor from steam reforming is adopted. Then, the reactor is cleaned by water and acetone before being reinstalled in the new system. And the dimension and setting of the reactor has been discussed in Chapter 3.

The schematic diagram of the experimental system for CO_2 reforming is shown in Ffigure 4.1. The three gas cylinders (hydrogen, carbon dioxide and methane) are connected directly into the reactor for different purposes. For each gas line, the check valves are installed to ensure no back flow. The Omega FMA 5400 gas mass flow controller is adopted to measure the flow rate for each gas. Compared to traditional flow meter, the electronic flow controller can maintain more constant flow and more precise flow rate. The flow rate is easily read from a LCD display. The reading from display is calibrated standard in SCCM or SLM for nitrogen. For methane and carbon dioxide, conversing calibration from standard gas is needed.

The two kinds of feed gas directly mixed at the inlet of reactor. After exiting from outlet of the reactor, the product gas is send to sampling loop in the GC system. A sampling controlled by a computer takes a certain amount product gas to make the result reproducible. The heating system and PID control group is remained same setup in the steam reforming experiment.

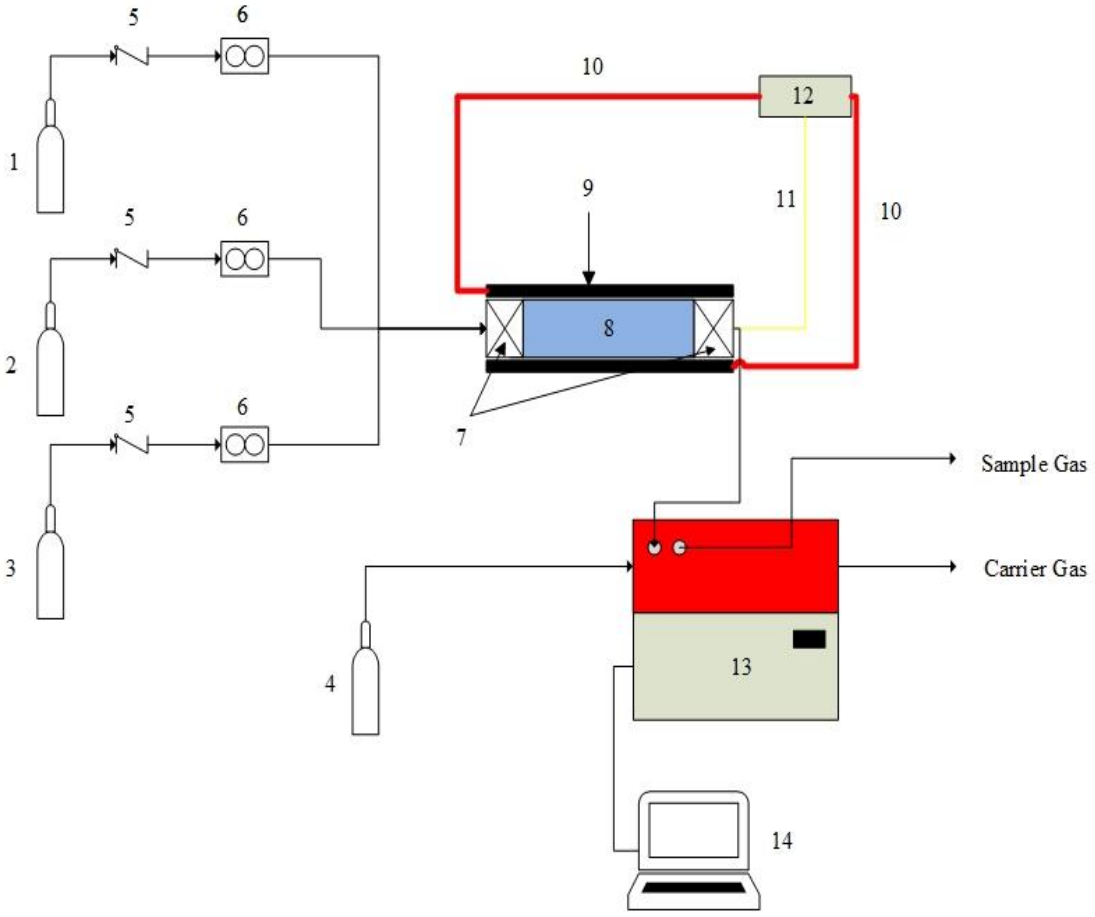

Figure 4.1 Schematic Diagram of CH_4-CO_2 Reforming Experiment

1. H_2 Cylinder 2. CH_4 Cylinder 3. CO_2 Cylinder 4. He Cylinder 5. Check Valve 6. Mass Flow Controller 7. SiO_2 8. Catalyst Bed 9. Ceramic Insulator 10. Ceramic Heating Wire 11. Thermal Couple 12. PID Controller System 13. GC System 14. Laptop

4.4 Experimental Procedure

After the experiment system setup, the leakage examination is conducted to prevent harzardous gas escaping from gas line and ensure exhaust into the ventilation system for laboratoary safety.

The single tunnel, fixed-bed reactor is used for catalytic test at atomsphere pressure. The amount of Ni/SiO_2 catalyst loaded in the reactor is 2.6g with 10% weight percentage of Ni. The molar ratio of CH_4:CO_2 for the mixture gas is 1:1, and total flow rate is 65 sccm. The reactor is wrapped with ceramic heating coil and covered ceramic insulation to keep temperature constant. The heating system is controlled by a PID controller to keep a stable heating rate, and a Type-K thermal couple is insert to monitor the temperature at catalyst bed.

The catalyst is reduced before the experiment to change metal oxides to activate metal form. The active sites of catalyst are created and enhanced through this thermal treatment process [77]. The heating process was controlled by a PID controller in a stepping process. The catalyst bed was preheated to 200° C with a H_2 flow at 50 sccm and holding the temperature for 30 min. Then the temperature is increased to 550° C with a constant heating rate 10℃/min under H_2 flow at 50 sccm for 4 hours.

The product gas from reactor is sent into the GC system (SRI Model 8610C) for composition analysis at room temperature. Gas Chromatograph (GC) is equipped a thermal conductivity detector to identify gas composition by measuring peak area from Peal Simple software.

The catalyst characterization was performed at the UTA Characterization Center for Materials & Biology using scanning electron microscopy (SEM) and X-ray diffractometer

(XRD). Bruker D8 Advance X-ray diffractometer was used for catalyst composition investigation. The sample of catalyst is grinded into fine powder, and the powder is compacted in a shallow well of a sample holder. The sample plate is fixed at XRD analysis platform. The 2-Theta range is chosen from 10˚ to 80˚ at a rate of 6˚ /min. The Hitachi S-5000H cold Field Emission SEM instrument is employed to observe the microstructure of catalyst and record digit image.

4.5 Experimental Data Process

The target reaction for CO_2 reforming process is shown in Eq. 4.1.

$$CH_4 + CO_2 \leftrightarrow 2CO + 2H_2 \qquad (4.1)$$

The calculations for conversion rate of reactant gas and yield rate of product gas from this reaction are listed below. The concentration for each gas component form GC is adopted in calculations.

Methane conversion: $$X_{CH_4} = \frac{[CH_4]_{(in)} - [CH_4]_{(out)}}{[CH_4]_{(in)}} \times 100\% \qquad (4.2)$$

Carbon dioxide conversion: $$X_{CO_2} = \frac{[CO_2]_{(in)} - [CO_2]_{(out)}}{[CO_2]_{(in)}} \times 100\% \qquad (4.3)$$

Hydrogen yield: $$Y_{H_2} = \frac{[H_2]_{(out)}}{2 * ([CH_4]_{(in)} - [CH_4]_{(out)})} \times 100\% \qquad (4.4)$$

Carbon monoxide yield: $$Y_{CO} = \frac{[CO]_{(out)}}{([CH_4]_{(in)} + [CO_2]_{(in)}) - ([CH_4]_{(out)} + [CO_2]_{(out)})} \times 100\% \qquad (4.5)$$

Where X and Y are conversion and yield, respectively.

4.6 Experimental Results

4.6.1 Effect of Temperature

The temperature range was set from 500℃ to 700℃ for the dry reforming experiment. Because the dry reforming is an endothermic reaction, as the rising temperature, the conversion rate also increases. From figure 4.2, the effect of temperature on CH_4 conversion rate is illustrated to evaluate the performance of experiment. The highest conversions rate 90.0 % is located at the temperature of 700℃, which is the highest setting temperature. While the temperature increase, the conversion rate of CO_2 also rises from 39.1% to 61.5%. The conversion rate of CO_2 versus temperature is presented in Figure 4.3. The rising temperature leads to conversion rate increase by 28.6% for CH_4 and 57.3% for CO_2. Consequently, since the main reaction is an endothermic process, high temperature has great benefit for increasing reaction efficiency. H_2/CO ratio is also influenced by changing temperature. The H_2/CO ratio is close to 1 according to stoichiometric number for product from dry reforming reaction. Figure 4.4shows that H_2/CO ratio of product gas increase with reaction temperature rising, and the ratio is slightly larger than 1. A possible reason for this phenomenon is that methane cracking reaction (Eq.4.7) occurs with the main reaction.

$$CH_4 + CO_2 \leftrightarrow 2CO + 2H_2,\ \Delta H = +247\ kJ/mol \qquad (4.6)$$

$$CH_4 \leftrightarrow C + 2H_2,\ \Delta H = +75\ kJ/mol \qquad (4.7)$$

From above equations, the dry reforming reaction and methane cracking reaction are both highly endothermic reactions. Therefore, the environment with high temperature can stimulate the conversion from these two equations. The H_2/CO ratio of product could be adjusted by post-process step to fulfill the F-T synthesis requirement.

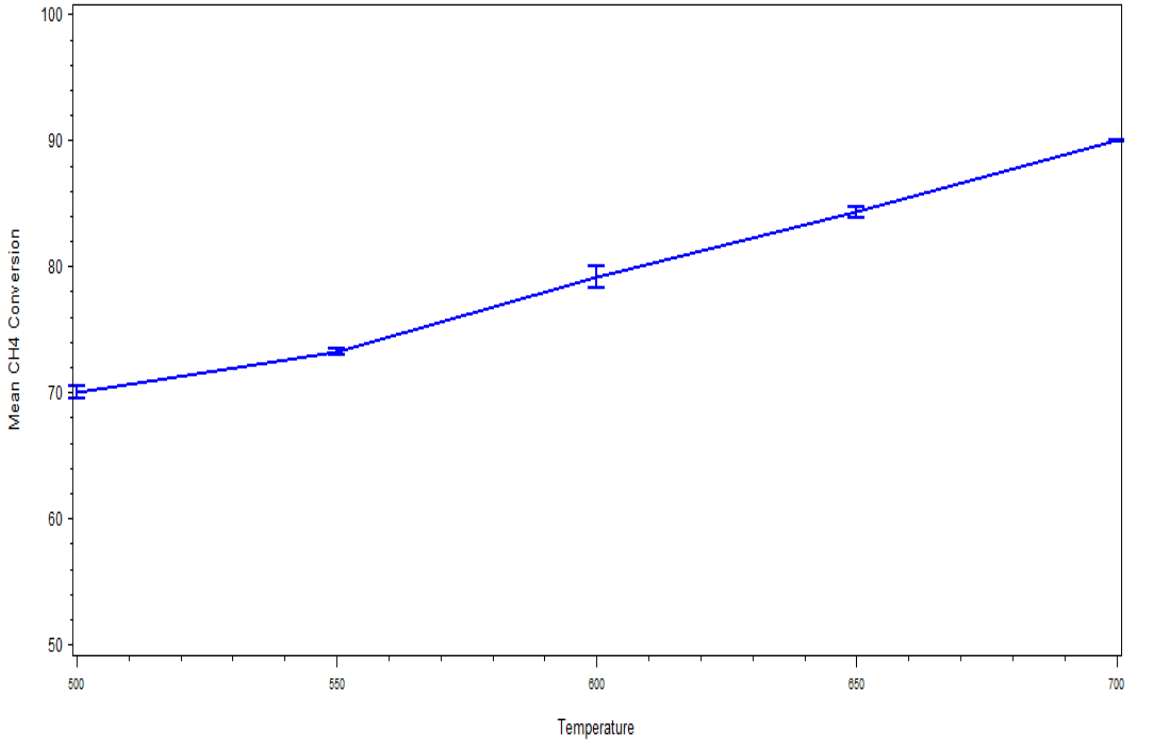

Figure 4.2 CH_4 conversion as a function of Temperature

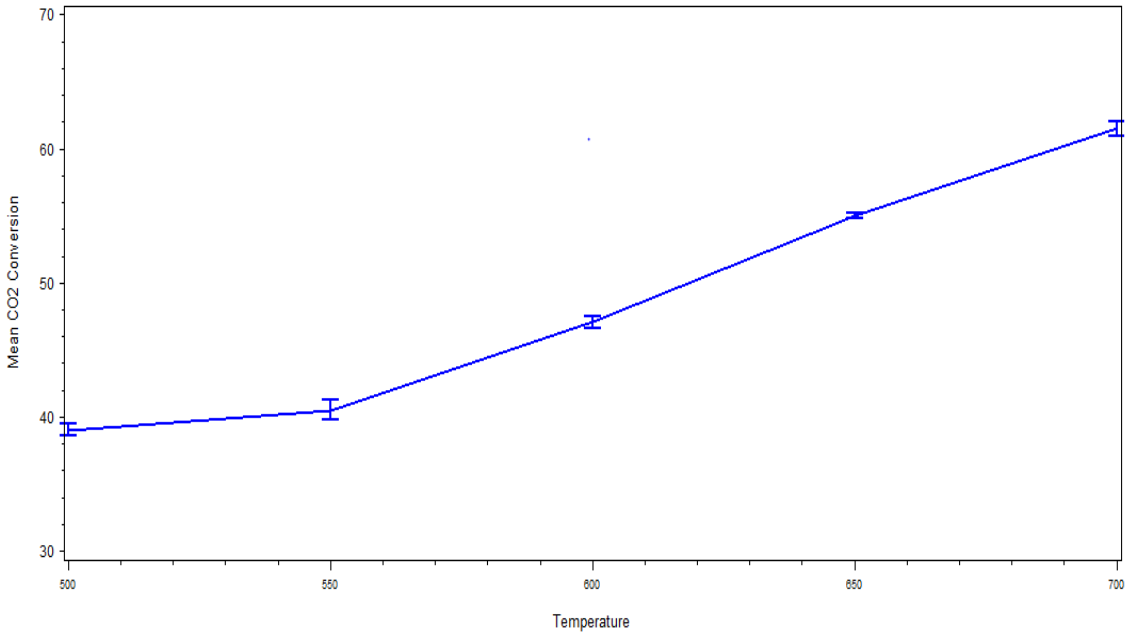

Figure 4.3 CO_2 conversion as a function of Temperature

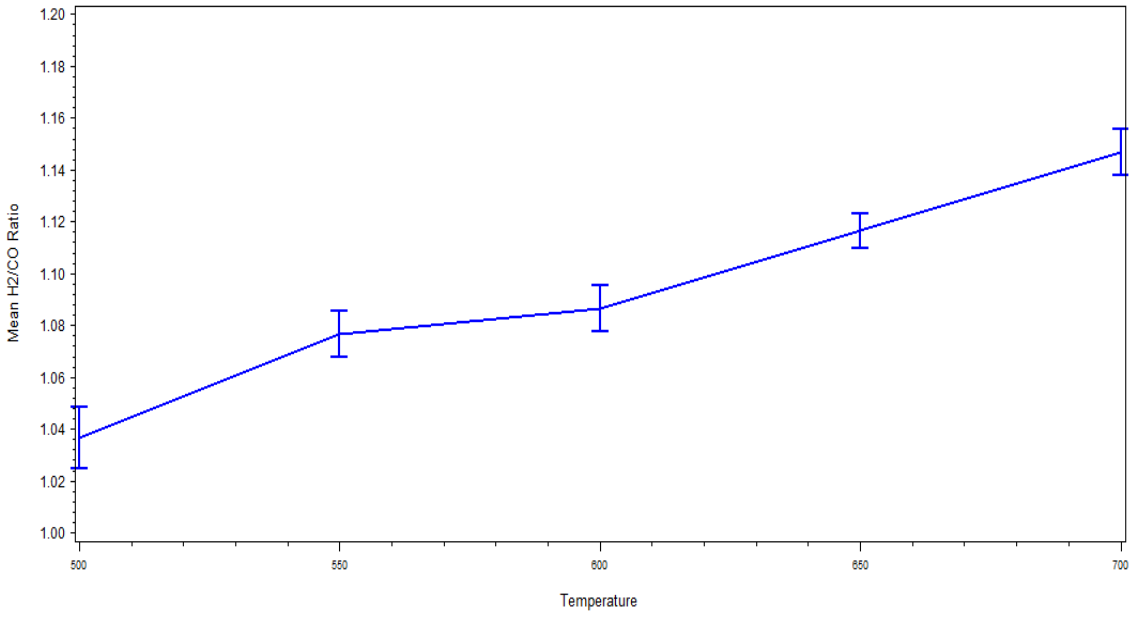

Figure 4.4 H_2/CO ratio as a function of Temperature

4.6.2 Characterization of Catalyst

In this study, the Ni/SiO_2 is characterized by two methods, XRD and SEM, to analysis carbon formation during the experiment. Because carbon deposition on the surface is main reason to cause Ni catalyst deactivation, a lot of study dedicate to resist carbon formation [78-80]. The CO_2 reforming has a more sever carbon formation than conventional steam reforming due to rich carbon element from reactant gases.

The XRD patterns for fresh Ni catalyst sample (Fig.4.5), Ni catalyst sample after reduction (Fig.4.6) and Ni catalyst sample after reaction (Fig.4.7) are listed below for comparison. In the XRD pattern of fresh Ni catalyst, the Ni is in two types of existence, metal site and metal oxide site. The presence of Ni oxide is detected from two peaks, which are strong peak at $2\theta=37.1^\circ$ and weaker one at $2\theta=62.9^\circ$. Therefore, reduction of catalyst is necessarily conducted to transfer metal oxide to active metal. After reduction, the Ni oxide peak is no longer visible from XRD patterns, as shown in Figure 4.6. The catalyst is conducted under H_2 flow at 550℃ for 4 hours. Compared to fresh catalyst in Figure 4.5, only catalyst and catalyst support are observed from XRD pattern, and the intensity of Ni catalyst increases from transformation of NiO. In the Figure 4.7, the high intensity diffraction peak is detected at $2\theta=26.4^\circ$ for the catalyst sample. The peak indicates the carbon presence in the catalyst. Although the catalyst was still active after 60~80 hours'

experiment, the accumulation of carbon deposition on the catalyst will cause catalyst deactivation gradually for long term running in the fixed bed reactor.

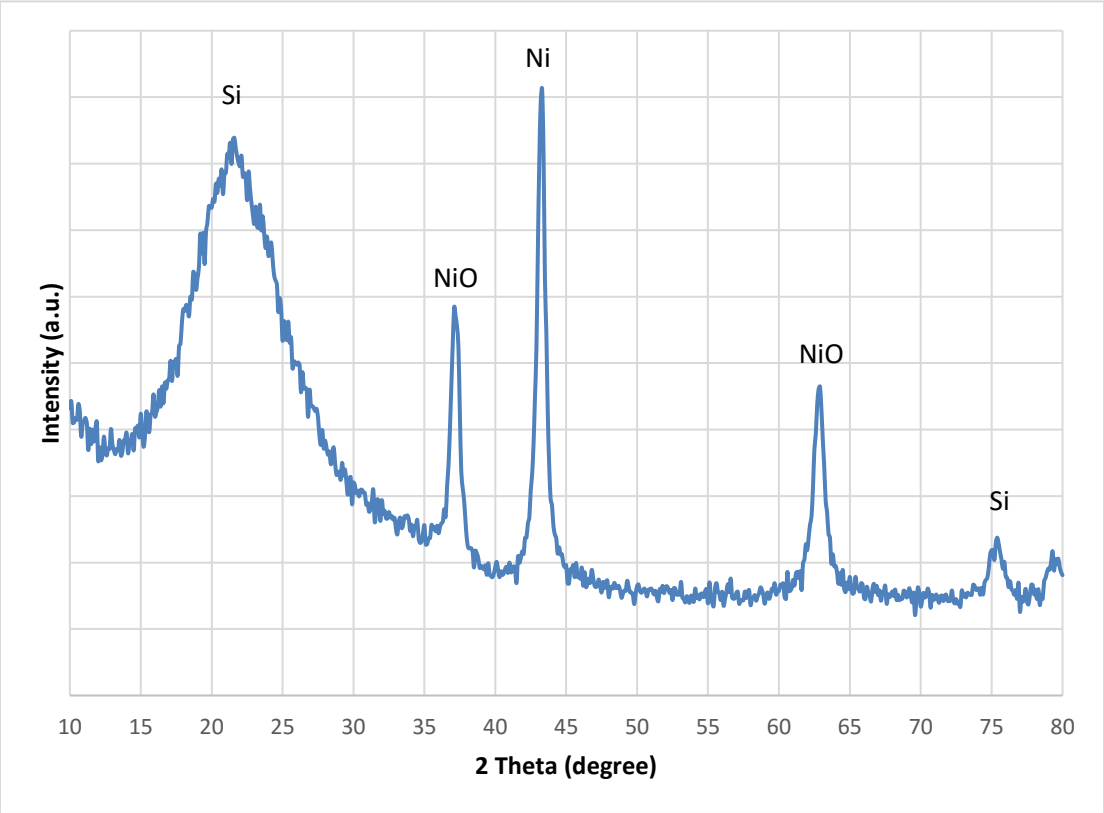

Figure 4.5 XRD pattern of fresh Ni/SiO_2 catalyst

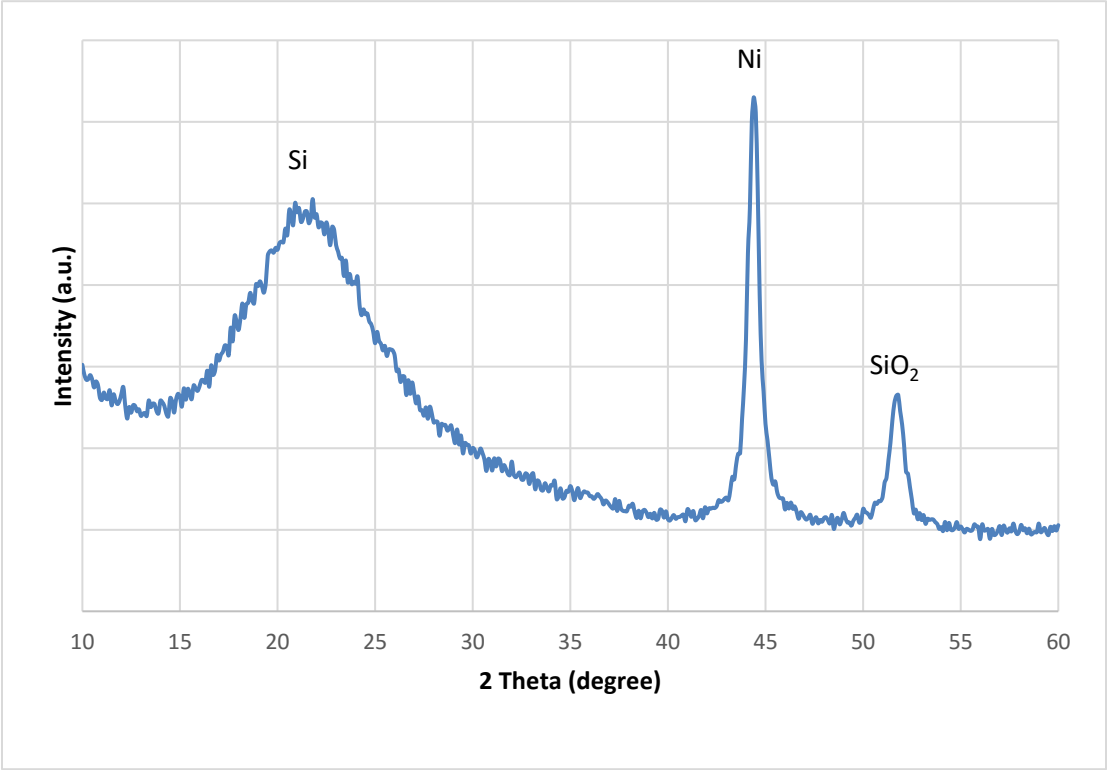

Figure 4.6 XRD pattern of Ni/SiO_2 catalyst after reduction

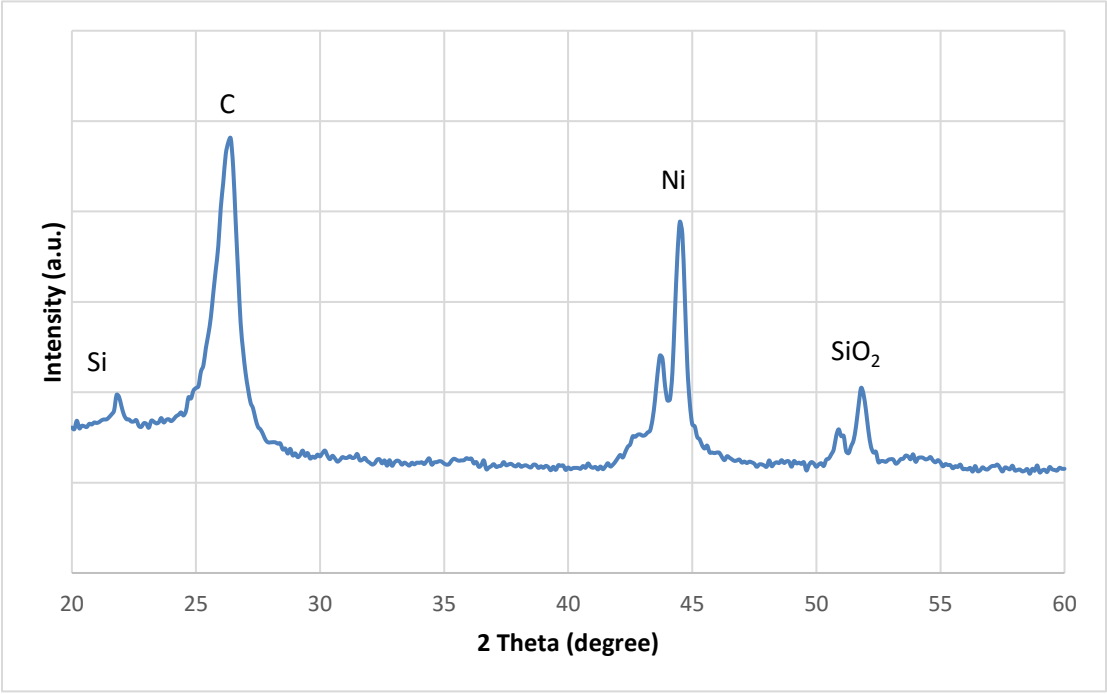

Figure 4.7 XRD pattern of Ni/SiO_2 catalyst after reaction

The catalyst was examined by SEM to investigate the morphology in the three different phases in the Figure 4.8~4.10. It is observed that the Ni is deposited on the catalyst by impregnation method in Figure 4.8. The Ni covers most of surface on the catalyst, but there are still some uncovered area and other substance on the surface. Compared to fresh catalyst, the micrograph of catalyst (Figure 4.9) after reduction shows a clean and uniform active site. Carbon deposition is confirmed at catalyst after reaction from Figure 4.10. In Figure 4.10 (a), a single filamentous pillar is illustrated in the picture, which is an evidence for graphitic carbon existence. [49] And in Figure 4.10 (b), the surface of active catalyst is covered by a large amount of such pillar. Therefore, the observed phenomenon from SEM image indicates that carbon deposition on the catalyst damage the activation site of catalyst and eventually lead to deactivation in dry reforming reaction.

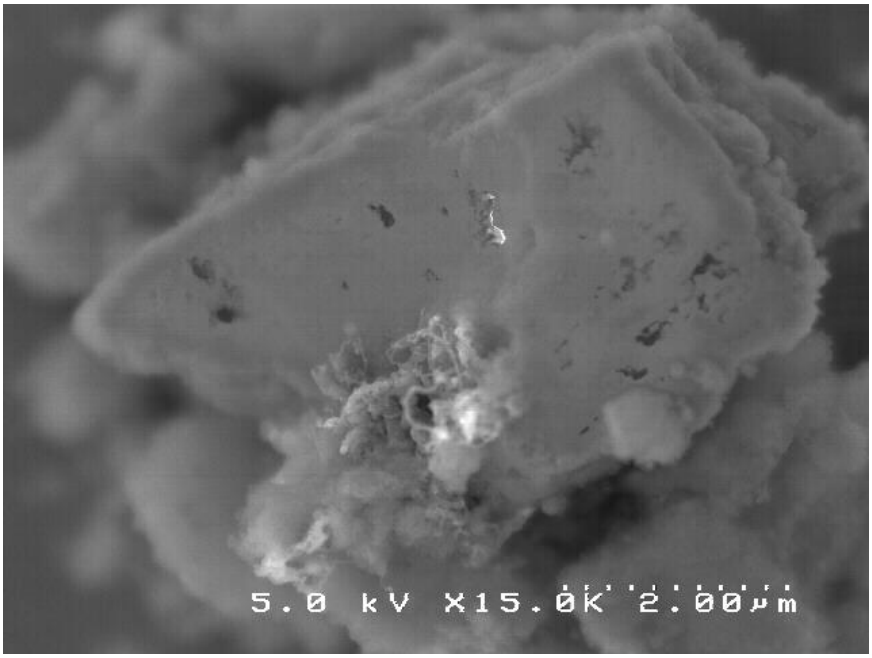

Figure 4.8 SEM image of fresh Ni/SiO_2 catalyst

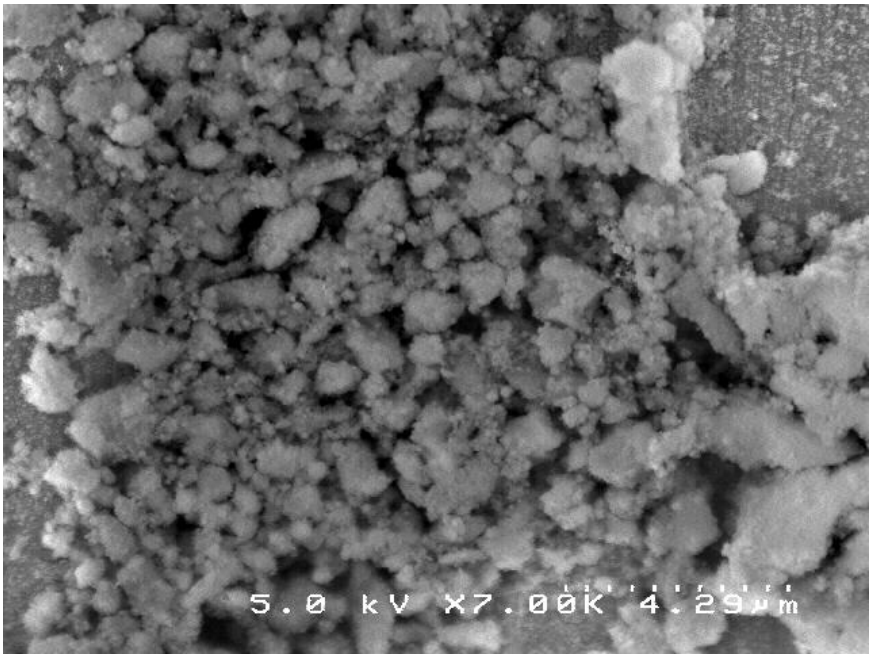

Figure 4.9 SEM image of Ni/SiO_2 catalyst after reduction

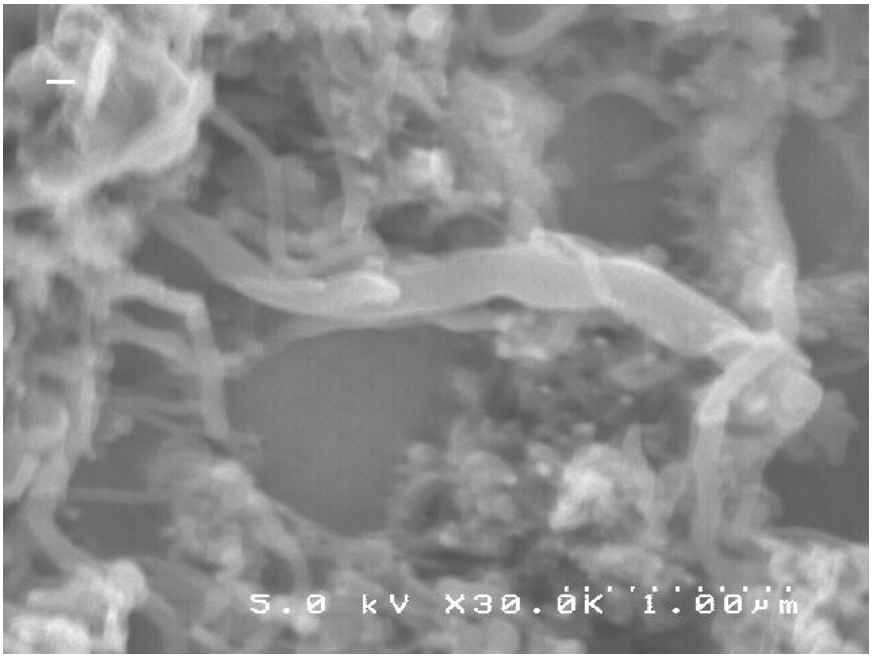

(a)

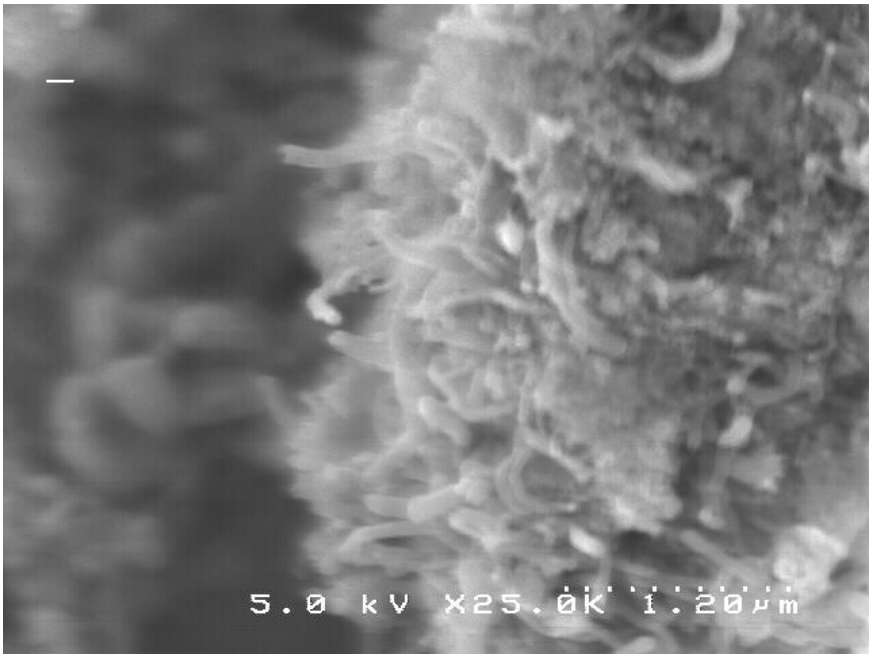

(b)

Figure 4.10 SEM image of Ni/SiO_2 catalyst after reaction (a) Carbon Pillar

(b) Ni catalyst covered by Carbon

4.7 Catalyst Stability Test

Based on the experiment setup of CO_2 reforming, a long term test for Ni/SiO_2 was performed to testify stability. The Ni/SiO_2 was prepared using impregnation method. The experiment was conducted at 700° C with total flow rate 65 sccm. The 2.70-gram Ni/SiO_2 (Ni 10% wt.) was loaded in the reactor. The experiment was operated in a high carbon intensity with a CO_2/CH_4 ratio 4 for carbon resistant ability test of catalyst. At this CO_2/CH_4 ratio, beside methane cracking (Eq. 4.8) and Boudouard reaction (Eq. 4.9), the carbon is also produced from Equation 4.10.

$$CH_4 \leftrightarrow C + 2H_2 \qquad (4.8)$$

$$2CO \leftrightarrow CO_2 + C \qquad (4.9)$$

$$CO_2 + 2H_2 \leftrightarrow C + 2H_2O \qquad (4.10)$$

The catalytic performance is described in terms of the CH_4 conversion and the CO_2 Conversion, as shown in Figure 4.7. In Figure 4.7, the conversion rate of methane reached at over 99% for long time, in contrast to decrease conversion rate of carbon dioxide. Compared to results at CO_2/CH_4 ratio 1, the conversion rate of methane increases as long as carbon dioxide decrease. The reason for decrease conversion for CO_2 is not only because of catalyst deactivation, but the excess amount of CO_2 in the reaction cause reverse water gas shift reaction in the reactor. Since the major product from RWGS is CO and H_2O, the steam from RWGS and carbon is reacted to generate syngas through coke gasification

reaction. Because ΔH in SMR is less than dry reforming, the conversion of CO_2 is depressed. For the catalyst, even if the conversion rate for CO_2 is zero, the product gas sample contains hydrogen and carbon monoxide after 24-hour running. However, the H2/CO ratio is less than 1 because of side reaction of RWGS. The conversion rate of methane keeps at a high level for a long term in this experiment. It is indicated that the catalyst is able to support CO_2 Reforming for a long term running, and the ratio of CO_2/CH_4 need to be choose wisely to avoid side reaction and keep high conversion for reactant gas.

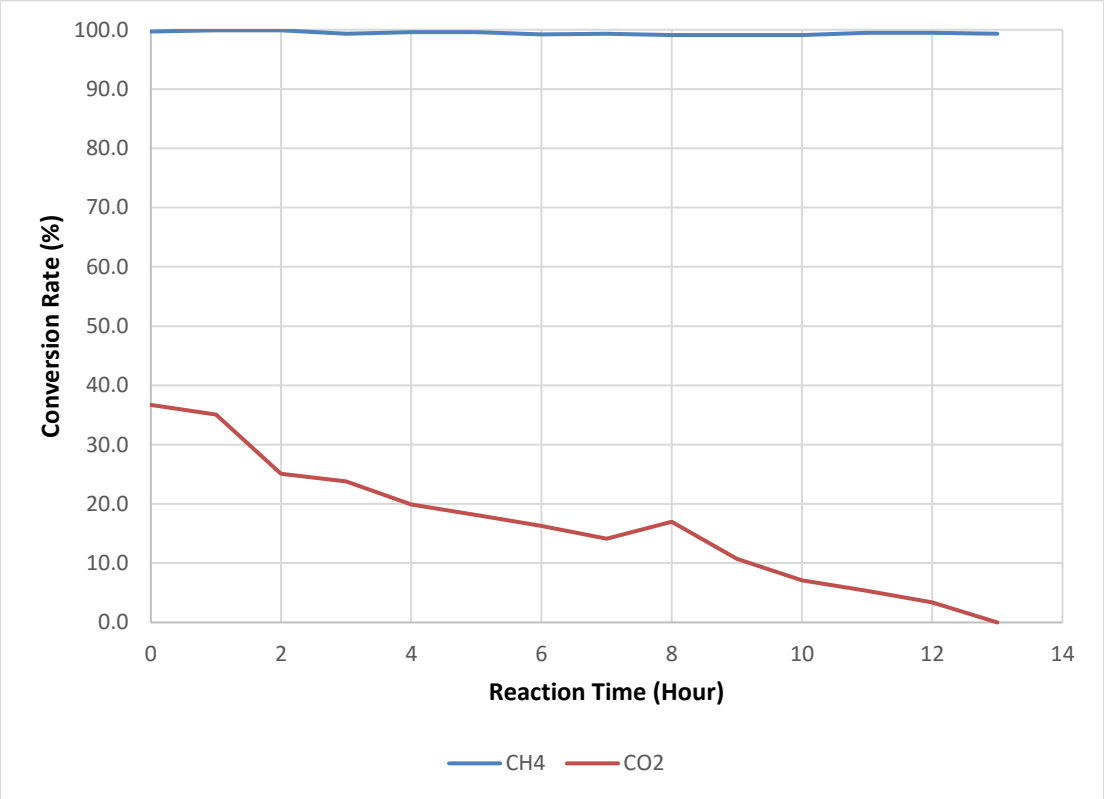

Figure 4.11 Conversion Rate for Stability Test

4.8 Comparison of Steam Reforming and Dry Reforming

Steam Methane Reforming and Dry Reforming are two promising methods for syngas production. Based on previous research and this study, there are several advantages and disadvantages for each reforming method.

First, compared to the Dry Reforming, the experiment for SMR requires an extra device for steam generation from liquid water. Although extra device increases the risk of leakage and maintenance cost, the steam in the reactor not only acts as reactant gas but effectively reduces the carbon formation during reforming reaction. The excess steam is involved in coke gasification reaction (Eq. 4.11) to help transfer carbon on the catalyst surface to syngas. In contrast, the dry reforming has high carbon concentration, which easily lead to carbon formation in the reactor. From the XRD patterns for each reforming process, the intense of C from dry reforming is higher than steam reforming after long period running (60~80 hours). And the active part of catalyst, Ni, has a stronger intense from steam reforming reaction.

$$C + H_2O \leftrightarrow CO + H_2, \Delta H = +131 \text{ kJ /mol} \qquad (4.11)$$

Second, the most attractive point for dry reforming is that, two major greenhouse gases are using as feedstock to produce syngas. Based on high conversion rate in this study, this feature offers an alternative method to reduce emission of greenhouse gas. Even if the dry

reforming reaction required more enthalpy than steam reforming reaction, which requires more heat for reaction, the conversion rate for methane is higher at same temperature.

Moreover, the syngas product has different H_2/CO ratio from each reaction process. The product ratio for steam reforming reaction is close to 3, compared 1 from dry reforming. For liquid fuel production by Fischer-Tropsch process, the desirable H_2/CO ratio is around 2~3 based on stoichiometric number of F-T process. Therefore, the product syngas of steam reforming is more suitable for directly application in F-T process. However, combined product from 2 reforming method can control H_2/CO ratio from 1 to 3, which may meet further requirement for research of synthesis fuel production.

4.9 Summary

The CO_2 reforming system is investigated in this chapter. The experiment system is modified from SMR experiment. The results from this experiment shows that temperature is a crucial parameter on the performance of reaction because dry reforming is a strong endothermic process. The reaction temperature can affect both reactant gas conversion rate and composition of product gas. The product gas has a lower H_2/CO than SMR reaction, which is close to 1. The higher temperature leads to higher conversion rate, the highest conversion rate for CH_4 and CO_2 are 90.0% and 61.5% at 700° C.

The carbon deposition is also discussed in this chapter. The carbon formation is from following two reactions: $CH_4 \leftrightarrow C + 2H_2$ and $2CO \leftrightarrow CO_2 + C$. The catalyst in three phases

(fresh, reduced, after reaction) has been examined by XRD and SEM method. The XRD patterns reveals the effect of reduction process to transform from metal oxide to active metal and increase the intensity of active metal, which are benefit for catalyst performance. The carbon diffraction peak is detected in the catalyst sample after reaction. And from SEM image, the filamentous carbon is observed existing on the surface of catalyst from CO_2 reforming of CH_4. The carbon deposition on the catalyst might be the main reason for catalyst deactivation. Although Ni/SiO_2 could maintain activity for long period, as long as more filamentous carbon formed on the catalyst, the deactivation is inevitable.

The catalyst is placed in a rich carbon element environment for stability test. The Ni/SiO_2 is able to support syngas production for a long term even in a high carbon intensity condition. Through this experiment, it is revealed that the high reactant gas ratio of CO_2/CH_4 is not favored by CO_2 reforming of CH_4 because of a series of side reactions.

Chapter 5
NUMERICAL ANALYSIS

In this chapter, two models are built by COMSOL to discuss the performance for experiment setup. The kinetic rate of reactions and governing equations are presented. Furthermore, the results from numerical analysis will be discussed.

5.1 Model Introduction

The numerical models for 2 different reforming method are established and validated by using COMSOL. To compare the results of numerical analysis with experimental data, a 2-D model for a tubular reactor is developed with several assumptions. The reaction flow is assumed at steady state, and pressure of reactor is set at 1 bar. For the COMOSOL, the module, Laminar Flow, is applied to simulate reaction flow in tubular reactor. The dimension of reactor and catalyst bed is same as experiment.

The main purpose for the simulation, is to compare the product compositions with experiment's result. Matching previous results of experiment help experiment design validation. Meanwhile, using simulation for reforming process can be implement for experiment to examine various parameters on product composition and help modification and improvement of the reactor design to archive higher conversion rate. The study can also investigate the effect of combination for steam and dry reforming.

5.2 Governing Equation

By using Laminar Flow module in COMSOL, the gas flow in the reactor is assumed as incompressible, steady and laminar. The Naiver-Stokes equations, including continuity, momentum and species transport, are applied to solve velocity field in the reactor.

Continuity Equation

$$\nabla \cdot (\rho u) = 0 \quad (5.1)$$

Momentum Equation

$$\rho(u \cdot \nabla)u = \nabla \cdot [-pI + \mu(\nabla u + (\nabla u)^T) - \frac{2}{3}\mu(\nabla \cdot u)I] + F \quad (5.2)$$

Where, u is the velocity field (m/s)

ρ is the gas density (kg/m^3)

p is the pressure (Pa)

μ is the molecular viscosity (N·s/m^2)

F is the body force per volume (N/m^3)

Species transport Equation is applied to solve concentration distribution in the reactor for reforming process. The equation is given below.

$$\nabla \cdot j_i + \rho(u \cdot \nabla)\omega_i = R_i \quad (5.3)$$

Where, j_i is the diffusional flux of species i (kg/m^2·s)

ω_i is the mass fraction of species i

R_i is the rate of production of species i (kg/m^3·s)

The j_i, diffusional flux of species i, can be expressed in equation (5.4) by Maxwell-Stefan model.

$$j_i = -(\rho D_i^m \nabla \omega_i + \rho \omega_i D_i^m \frac{\nabla M_n}{M_n} + D_i^T \frac{\nabla T}{T}) \quad (5.4)$$

Where, D_i^m is the binary diffusivity coefficient (m^2/s)

$M_n = (\sum_i \frac{\omega_i}{M_i})^{-1}$, M_i is the molar mass of species i (kg/mol)

D_i^T is the thermal diffusivity coefficient (m^2/s)

T is the reactor temperature (K)

The binary diffusivity coefficient can be estimated from empirical equation by Chapman-Enskog theory in equation (5.5). [85]

$$D_{AB} = 0.0018583 \sqrt{T^3 (\frac{1}{M_A} + \frac{1}{M_B})} \frac{1}{p \sigma_{AB}^{\ 2} \Omega_{AB}} \quad (5.5)$$

Where, σ_{AB} is collision diameter ($\mathring{A}$), and can be calculated by $\sigma_{AB} = \frac{1}{2}(\sigma_A + \sigma_B)$

Ω_{AB} is the collision integral (K)

5.3 Kinetics for Reforming Reactions

The kinetic rate model developed by Xu and Froment [86] is applied for steam reforming simulation in the reactor. The reforming simulation conations three major reactions, including steam methane reforming reaction, water gas shift reaction, and global reaction. And the reaction rates for these reactions are listed in the equation (5.6) - (5.8).

$CH_4 + H_2O \leftrightarrow CO + 3H_2$ (Steam Reforming Reaction) reaction 1

$CO + H_2O \leftrightarrow CO_2 + H_2$ (Water Gas Shift Reaction) reaction 2

$CH_4 + 2H_2O \leftrightarrow CO_2 + 4H_2$ (Global Reaction) reaction 3

$$r_1 = \frac{k_1}{p_{H_2}^{2.5}} \frac{(p_{CH_4} p_{H_2O} - p_{CO} p_{H_2}^{3} / K_1)}{(DEN)^2} \quad (5.6)$$

$$r_2 = \frac{k_2}{p_{H_2}} \frac{(p_{CO} p_{H_2O} - p_{CO_2} p_{H_2} / K_2)}{(DEN)^2} \quad (5.7)$$

$$r_3 = \frac{k_3}{p_{H_2}^{3.5}} \frac{(p_{CH_4} p_{H_2O}^{2} - p_{CO_2} p_{H_2}^{4} / K_3)}{(DEN)^2} \quad (5.8)$$

Where, $DEN = 1 + K_{CH_4} p_{CH_4} + K_{CO} p_{CO} + K_{H_2} p_{H_2} + \frac{K_{H_2O} p_{H_2O}}{p_{H_2}}$

r_1, r_2, r_3 are rate of reaction 1, 2 and 3 (kmol /(kg cat·h))

p_j is partial pressure of component j (bar)

K_1, K_3 are equilibrium constants of reaction 1 and 3 (bar^2)

K_2 is equilibrium constants of reaction 2

k_1, k_3 are rate coefficient of reaction 1 and 3 (kmol·bar$^{1/2}$/(kg cat·h))

k_2 is rate coefficient of reaction 2 (kmol/(kg cat·h·bar))

K_{CH_4}, K_{CO}, K_{H_2} are adsorption constant for CH_4, CO and H_2 (bar^{-1})

K_{H_2O} is adsorption constant of H_2O

The rate coefficient could be calculated by Arrhenius equation (Equation 5.9), and the adsorption constant could be calculated by Van't Hoff equation (Equation 5.10). The preexponential factors $A(k_i)$ and $A(K_j)$, activation energy E_i, and enthalpy change ΔH_j are listed in Table 5.1.

$$k_i = A(k_i)\exp(-\frac{E_i}{RT}) \quad (5.9)$$

$$K_i = A(K_i)\exp(-\frac{\Delta H_i}{RT}) \quad (5.10)$$

Where, R is gas constant (kJ/kmol)

Table 5.1 Constant for Arrhenius and Van't Hoff equation [86]

Activation Energy	E_1	E_2	E_3	
kJ/mol	240.1	67.13	243.9	
Preexponential factors	$A(k_1)$	$A(k_2)$	$A(k_3)$	
$A(k_i)$	$4.225*10^{15}$	$1.955*10^{6}$	$1.020*10^{15}$	
Enthalpy Change	ΔH_{CO}	ΔH_{H2}	ΔH_{CH4}	ΔH_{H2O}
kJ/mol	-70.65	-82.90	-38.28	88.68
Preexponential factors	$A(K_{CO})$	$A(K_{H2})$	$A(K_{CH4})$	$A(K_{H2O})$
A(Kj)	$8.23*10^{-5}$	$6.12*10^{-9}$	$6.65*10^{-4}$	$1.77*10^{5}$

For dry steaming model, the kinetics are applied in the model developed by Richardson and Paripatyadar [87]. This model has two major reactions, Dry Reforming Reaction and

Reverse Water-Gas Shift Reaction. The equations of reaction rate are listed from equation (5.11) to (5.12).

$CH_4 + CO_2 \leftrightarrow 2CO + 2H_2$ (Dry Reforming Reaction)

$H_2 + CO_2 \leftrightarrow CO + H_2O$ (Reverse Water-Gas Shift Reaction)

$$r_1 = k_1[\frac{(K_{CH_4} p_{CH_4} K_{CO_2} p_{CO_2})}{(1 + K_{CH_4} p_{CH_4} + K_{CO_2} p_{CO_2})^2}] \quad (5.11)$$

$$r_2 = k_2 p_{CO_2} \quad (5.12)$$

Where, $k_1 = 1290 \times \exp[-102065/(R \times T)]$ (mol g cat^{-1} s $^{-1}$) [88]

$k_2 = 1.856 \times 10^{-5} \times \exp[-73105/(R \times T)]$ (mol Pa^{-1} g cat^{-1} s $^{-1}$) [88]

$K_{CH_4} = 2.63 \times 10^3 \times \exp[40684/(R \times T)]$ (Pa^{-1}) [88]

$K_{CO_2} = 2.64 \times 10^3 \times \exp[37641/(R \times T)]$ (Pa^{-1}) [88]

5.4 Conditions for Simulation Model

To simplify simulation model, several assumptions are defined and summarized below.

1. The reactor is in a steady-state condition;
2. The gas is treated as ideal gas;
3. The gas flow is laminar;
4. The gravity affection is neglected;

5. The velocity and temperature are uniform in the reactor.

The boundary conditions at the reactor wall is assume that the velocity equals to zero, and the outlet pressure is set to 1 bar. For the species transport equation, the initial concentration of feedstock is set based on experiment data.

5.5 Results and Discussion

The Model is created in COMSOL, and to simplify the simulation process, the model has been set as a stationary process. The complete mesh for the model consists of 12468 domain elements and 1390 boundary elements. The Figure 5.1 shows a segment mesh for the reactor.

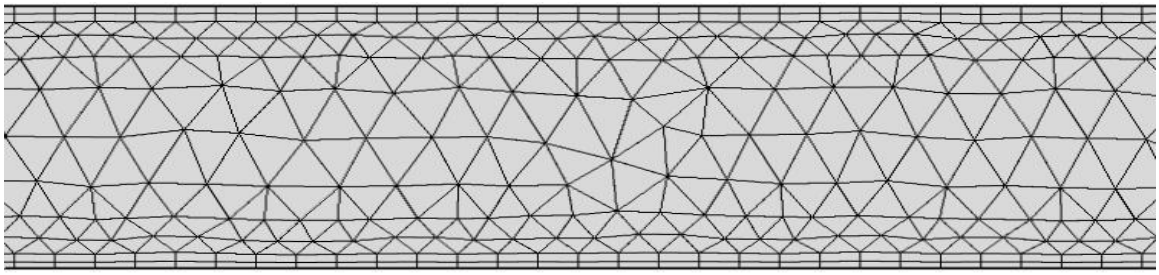

Figure 5.1 Mesh for Reactor

The fluid field in the reactor has been set as laminar flow and solved by laminar flow module in COMSOL. The fluid properties and initial values are chosen based on practical

experiment. The boundary conditions are set as no slip at the wall. For inlet, the average velocity is calculated from reactant gas flow rate and reactor section area. For outlet part, the suppress backflow has been applied. The flow field in the reactor is displayed in Figure 5.2.

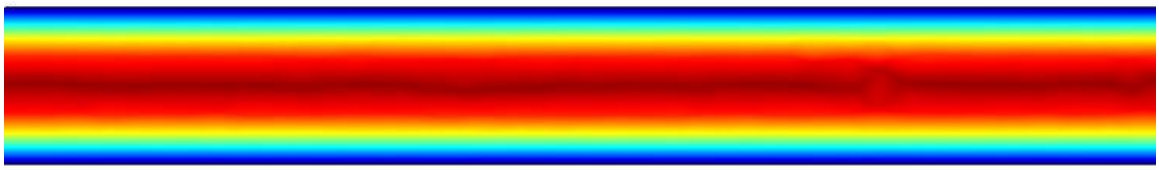

Figure 5.2 Laminar Flow in the Reactor

For steam reforming, as shown in Figure 5.3 and 5.4, the conversion rate of CH_4 increases and the H_2:CO ratio decrease with rising temperature. Because the simulation process has been simplified, the result has some difference with experiments. However, the results for both simulation and experiment state that the SMR process is boosted at a high temperature to reach a higher methane conversion rate and an appropriate product composition. Meanwhile, from simulation results, the effect of Steam/Carbon ratio is similar as experiments' results. From S/C ratio 1 to 4, the methane conversion rate is kept above 90%. However, the product H_2:CO ratio increases at high temperature, because the excess steam triggered the WGS reaction and increase H_2 production. Since our goal is to

produce syn-gas for F-T process, the higher ratio is not desirable. Therefore, the simulation results support our conclusion from Chapter 3.

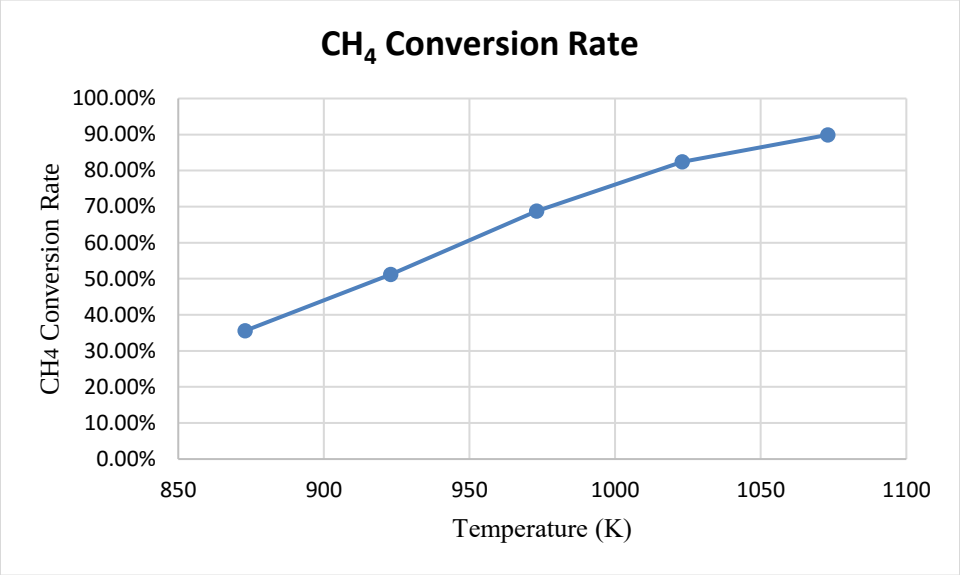

Figure 5.3 CH_4 Conversion Rate for Temperature (RSM)

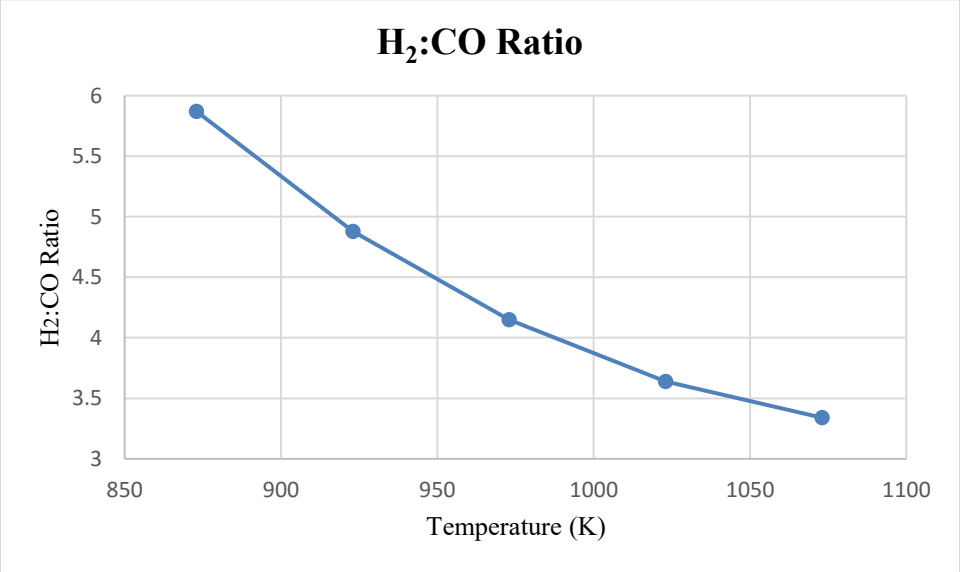

Figure 5.4 H_2O:CO Ratio for Temperature (RSM)

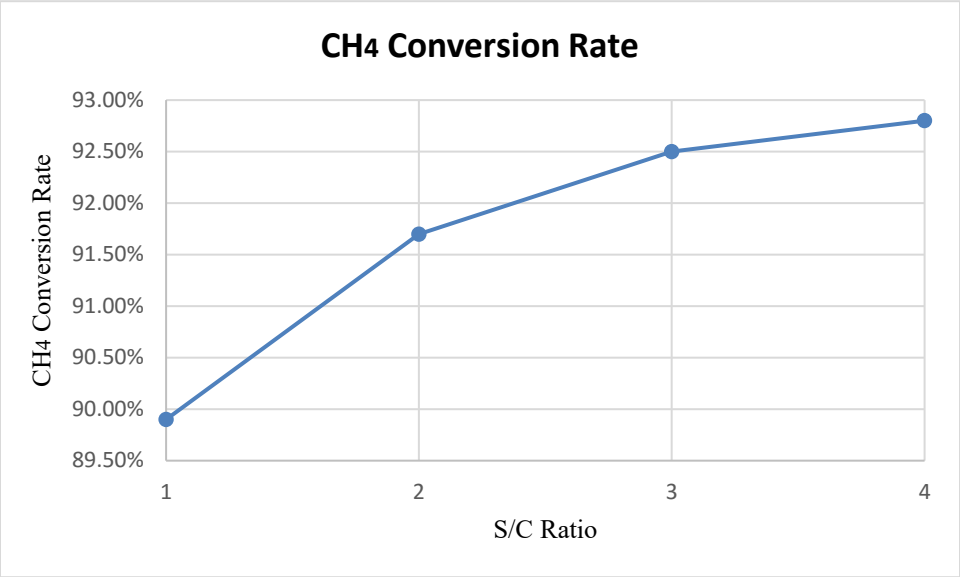

Figure 5.5 CH_4 Conversion Rate for S/C Ratio (RSM)

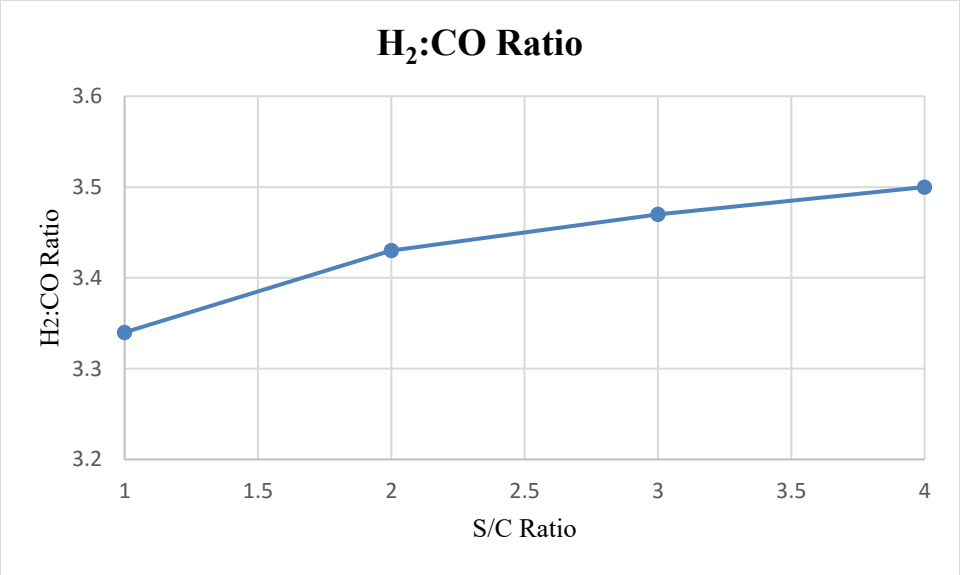

Figure 5.6 H_2O:CO Ratio for S/C Ratio (RSM)

For Dry reforming model, the main reaction has 2 parts, the dry reforming reaction and reverse WGS. In this model, the rate coefficient of the RWGS is quite low, so the reaction rate of the RWGS is much lower than the main reaction. Therefore, the product from the RWGS can be neglected, and the product composition (H_2: CO ratio) is majorly from the

main reaction, which is close to theoretical value, 1. As we discussed in Chapter 4, the dry reforming is an endothermic reaction. The higher temperature helps increase reaction efficiency. In Figure 5.7, the tendency of conversion rate is same as experiments. In the simulation process, we also test the different reactant ratios (CO_2:CH_4 ratio) to verify the experiments' result. The Figure 5.8 illustrates the CH_4 conversion rate versus CO_2:CH_4 ratio. From ratio 1 to 4, the conversion rate greatly drops because of excess CO_2 involved in the RWGS reaction. Moreover, the excess carbon element easily generates carbon, which could block the reactor and cover the activity surface of catalyst. Hence, from the simulation results, it shows that our experiments' setup is suitable for syn-gas production through Dry Reforming Reaction.

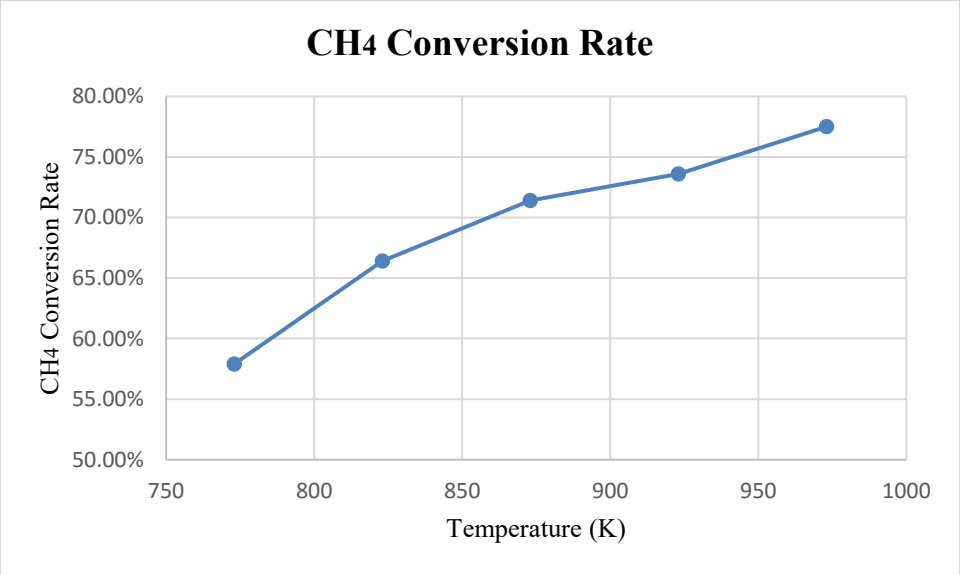

Figure 5.7 CH_4 Conversion Rate for Temperature (Dry)

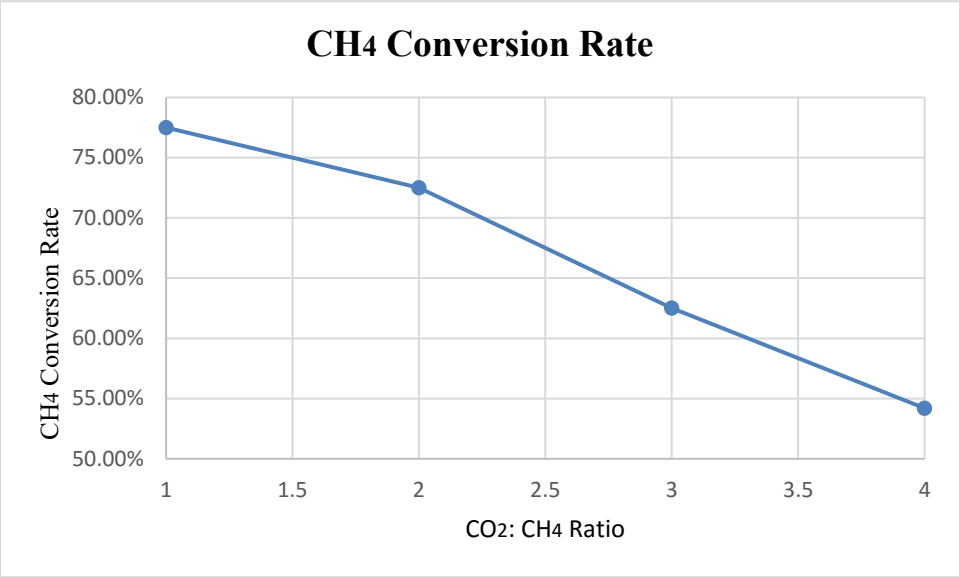

Figure 5.8 CH_4 Conversion Rate for CO_2:CH_4 Ratio (Dry)

Chapter 6
CONCLUSION AND FUTURE WORK

6.1 Conclusions

In this study, the major concern is to build a device, which supplies feedstock (syngas) for the Fischer-Tropsch synthesis process. Based on this purpose, two types of experiment are set up for the steam methane reforming and the CO_2 methane reforming. The experiments are investigated over Ni/SiO_2 catalyst in temperature range from 700˚ C to 800˚ C for SMR, and from 550˚ C to 700˚ C for dry reforming. High temperature is favored by reforming process because of endothermic property of reaction. The high conversation rate and proper composition of product gas are achieved at high temperatures. For SMR reaction, steam/methane (steam/carbon, S/C) ratio is another important parameter for reaction performance. The high S/C ratio is usually adopted in SMR to prevent carbon formation. However, if the S/C ratio is over high, the excess water steam reacts with CO through the water gas shift reaction (WGS). This method is normal for hydrogen production, but, for this study, the composition of product gas need to meet the requirement for F-T process. Therefore, the WGS reaction must be limited during the SMR reaction. The S/C ratio is optimized for this purpose at 3. For dry reforming, the ratio of CO_2/CH_4 is keep close 1 to depress unexpected side reactions. The Ni catalyst is able to active the two types reforming at high temperature for long time. After characterization by XRD and SEM

method, the carbon deposition has been found on the Ni catalyst at high temperature reaction condition which increases potential possibility for deactivation.

6.2 Recommendations for Future Work

The following recommendations for future work are summarized below:

1) Design a reactor with multi tunnels or dual tunnels that will greatly increase the efficiency of reaction. And combine dry reforming with steam reforming in the reactor. Because the H_2/CO ratio of product gas is high in the SMR and the H_2/CO ratio for dry reforming is lower. By combine these two reactions, the H_2/CO ratio could be adjusted by control the mixture ratio of reactant gas to meet downstream requirement without post –process step.

2) The effect of pressure in the reactor should be investigated. A lot of research reveals that pressure in the reactor has great effect on product yield and conversion of reactant gas [81~83]. Therefore, the influence of pressure could be involved in the future.

3) The catalyst with secondary active component could be applied in reforming reaction. The noble metal, added to Ni catalyst as secondary active component, could help improve catalyst stability and property of carbon resistant. And utilization of small amount of noble metal as additive will not greatly increase the cost for reforming.

4) The cost of energy should be estimated in the future. Because the reforming occurs at temperature over 700° C or higher. The cost and energy consumption for equipment maintenance at such a high temperature is tremendous. If the energy cost for reaction system exceed the value of product gas, the system will not be adopted in industry no matter how efficiency can be reached.

References

1. Robert Schlögl, Chemical Energy Storage, de Gruyter, Germany, 2013, 443.
2. United States Environmental protection Agency, Greenhouse Gas Emissions, Available: http://www.epa.gov/climatechange/ghgemissions/.
3. Reményi Károly, The Fossil-Fuels and the Global Warming, Journal of Energy and Power Engineering, 2012, 6,544-553.
4. Arun S.K. Raju, Chan S. Park, Joseph M. Norbeck, Synthesis gas production using steam hydrogasification and steam reforming, Fuel Processing Technology, 2009, 2,330-336.
5. R.P. O'Connor, E.J. Klein, L.D. Schmidt, High yields of synthesis gas by millisecond partial oxidation of higher hydrocarbons, Catalysis Letters, 2000, 3, 4,99-107.
6. DIFFER, MaSF - Materials and Materials Processing Technologies for Solar Fuels, Available: http://www.differ.nl/en/research/masf.
7. L. D'Alessio, M. Paolucci, Energetic aspects of the syngas production by solar energy: Reforming of methane and carbon gasification, Solar & Wind Technology, 1989, 2, 101-104.
8. Crabtree G., Dresselhaus M., Buchanan M., The hydrogen economy, Physical Today, 2004, 57, 39-44;

9. Wu J, Fang Y, Wang Y., Production of Syngas by Methane and Coal Co-Conversion in Fluidized Bed Reactor, International Workshop on Investment Opportunities in Coal Mine Methane Projects in China, 2000.
10. Sheldon R A., Chemicals from synthesis gas: catalytic reactions of CO and H_2, Springer, 1983.1.
11. Littlewood, K., Gasification: Theory and Application, Prog. Energy Combust. Sci., 1977, 3, 35-71.
12. Larminie J, Dicks A, McDonald M S. Fuel cell systems explained [M]. New York: Wiley, 2003.
13. A.P.E. York, T. Xiao, M.L.H. Green, and J.B. Claridge, Catalysis Reviews 2007, 49, 511–560.
14. Pena, M.A., Gomez, J.P., and Fierro, J.L.G., New catalytic routes for syngas and hydrogen production, Appl. Catal. A, 1996, 144, 7-57.
15. Gadalla, A.M. and Bower, B., The role of catalyst support on the activity of nickel for reforming methane with CO_2, Chem. Eng. Sci., 1988, 43, 3049-3062.
16. A. Berman, R.K. Karn, M. Epstein, Kinetics of steam reforming of methane on Ru/Al_2O_3 catalyst promoted with Mn oxides, Applied Catalysis A: General, 2005, 282,73–83;
17. J.P. Van Hook, Methane-Steam Reforming, Catalysis Reviews: Science and Engineering, 1980, 21,1–51;

18. J.R. Rostrub Nielson, D.L. Trimm, Mechanisms of carbon formation on nickel-containing catalysts, Journal of Catalysis, 1977, 48,155-165;
19. L.S. Lobo, D.L. Trimm, J.L. Figueiredo, in: Proceedings of the Fifth International Congress on Catalysis, 1972, Palm Beach, North Holland/American Elsevier, 1973, 2, 1125;
20. Bradford, and M.C.J., Vannice, M.A., CO_2 reforming of CH_4, Catal. Rev. Sci. Eng, 1999, 41, 1.
21. M. A. Gerber, Review of Novel Catalysts for Biomass Tar Cracking and Methane Reforming, Prepared for the U.S. Department of Energy, 2007.
22. Berman A, Karn R K, Epstein M. Kinetics of steam reforming of methane on Ru/Al_2O_3 catalyst promoted with Mn oxides [J]. Applied Catalysis A: General, 2005, 282(1): 73-83.
23. Fischer F., Tropsch, H., Uber die Herstellung synthetischer ¨olgemische (Synthol) durch Aufbau aus Kohlenoxyd und Wasserstoff, Brennstoff-Chem, 1923, 4,276–285.
24. Jager, B.; Espinoza, R., Advances in low-temperature Fischer-Tropsch synthesis, Catal. Today 1995, 23, 17–28.
25. Fox, III, J.M., The different catalytic routes for methane valorization: an assessment of processes for liquid fuels, Catal. Rev.-Sci. Eng. 1993, 35, 169–212.

26. Choi G N, Kramer S J, Tam S, et al, Design/Economics of a Once-Through Natural Gas Fischer-Tropsch Plant With Power Co-Production[C]//Coal Liquefaction & Solid Fuels Contractors Review Conference. 1997.
27. F. Marschner, H.J. Renner, and W. Boll, Ullmann's Encyclopedia of Industrial Chemistry, Wiley-WCH, Weinheim, 2007, 21-39.
28. Aguilera R F. The future of the European natural gas market: A quantitative assessment [J], Energy, 2010, 35(8), 3332-3339.
29. V. Subramani, P. Sharma, L. Zhang, K. Liu, and C. Song, Hydrogen and Syngas Production and Purification Technologies: Hydrocarbon Processing for H2 Production (Eds. K. Liu, C. Song, V. Subramani), Wiley, New-York, 2010, 14-126.
30. Elshout R. Hydrogen production by steam reforming [J]. Chemical engineering, 2010, 117(5), 34-38.
31. Schrope M., Which way to energy utopia?, Nature, 2001, 4, 414-682.
32. Bustamante F, Enick R, Rothenberger K, et al. Kinetic study of the reverse water gas shift reaction in high-temperature, high-pressure homogeneous systems [J]. Fuel Chem. Div. Preprints, 2002, 47.
33. Tingey G L, Kinetics of the Water—Gas Equilibrium Reaction. I. The Reaction of Carbon Dioxide with Hydrogen [J], The Journal of Physical Chemistry, 1966, 70(5), 1406-1412.

34. Wu H, La Parola V, Pantaleo G, et al. Ni-Based Catalysts for Low Temperature Methane Steam Reforming: Recent Results on Ni-Au and Comparison with Other Bi-Metallic Systems [J], Catalysts, 2013, 3(2), 563-583.
35. Edwards, J.H., Maitra, A.M. The chemistry of methane reforming with carbon dioxide and its current and potential applications, Fuel Process, Technol, 1995, 42, 269–289.
36. Rostrup-Nielsen J R, Sulfur-passivated nickel catalysts for carbon-free steam reforming of methane [J], Journal of Catalysis, 1984, 85(1), 31-43.
37. Song X, Guo Z, Technologies for direct production of flexible H2/CO synthesis gas [J], Energy Conversion and Management, 2006, 47(5), 560-569.
38. ST C T, NEUMANN P, VON LINDE F, The CALCOR Standard and CALCOR Economy Processes [J], OIL GAS European Magazine, 2001, 45.
39. Bartholomew C H, Mechanisms of catalyst deactivation [J], Applied Catalysis A: General, 2001, 212(1), 17-60.
40. Rostrup-Nielsen J R, Sehested J, Nørskov J K, Hydrogen and synthesis gas by steam- and CO2 reforming [J], Advances in catalysis, 2002, 47, 65-139.
41. Ramallo-López J M, Requejo F G, Craievich A F, et al, Complementary methods for cluster size distribution measurements: supported platinum nanoclusters in methane reforming catalysts [J], Journal of Molecular Catalysis A: Chemical, 2005, 228(1), 299-307.

42. Yokota S, Okumura K, Niwa M, Support effect of metal oxide on Rh catalysts in the CH_4-CO_2 reforming reaction [J], Catalysis letters, 2002, 84(1-2), 131-134.

43. Wei J, Iglesia E, Structural requirements and reaction pathways in methane activation and chemical conversion catalyzed by rhodium [J], Journal of Catalysis, 2004, 225(1), 116-127.

44. Hou Z, Chen P, Fang H, et al, Production of synthesis gas via methane reforming with CO_2 on noble metals and small amount of noble-(Rh-) promoted Ni catalysts [J], International journal of hydrogen energy, 2006, 31(5), 555-561.

45. Zhang Z L, Tsipouriari V A, Efstathiou A M, et al, Reforming of methane with carbon dioxide to synthesis gas over supported rhodium catalysts: I. Effects of support and metal crystallite size on reaction activity and deactivation characteristics [J], Journal of Catalysis, 1996, 158(1), 51-63.

46. Mark M F, Maier W F, CO_2-Reforming of Methane on Supported Rh and Ir Catalysts [J], Journal of Catalysis, 1996, 164(1), 122-130.

47. Erdohelyi A, Cserenyi J, Solymosi F, Activation of CH_4 and Its Reaction with CO_2 over Supported Rh Catalysts [J], Journal of Catalysis, 1993, 141(1), 287-299.

48. Xu J, Froment G F, Methane steam reforming, methanation and water-gas shift: I. Intrinsic kinetics [J]. AIChE Journal, 1989, 35(1), 88-96.

49. Hao Z, Zhu Q, Lei Z, et al, CH_4–CO_2 reforming over Ni/Al_2O_3 aerogel catalysts in a fluidized bed reactor [J], Powder Technology, 2008, 182(3), 474-479.

50. Hao Z, Zhu Q, Jiang Z, et al, Characterization of aerogel Ni/Al_2O_3 catalysts and investigation on their stability for CH_4-CO_2 reforming in a fluidized bed [J]. Fuel processing technology, 2009, 90(1), 113.
51. Jing Q, Lou H, Mo L, et al, Comparative study between fluidized bed and fixed bed reactors in methane reforming with CO_2, 459-469.
52. Meshkani F, Rezaei M, Nickel catalyst supported on magnesium oxide with high surface area and plate-like shape: a highly stable and active catalyst in methane reforming with carbon dioxide [J], Catalysis Communications, 2011, 12(11), 1046-1050.
53. Effendi A, Zhang Z G, Hellgardt K, et al, Steam reforming of a clean model biogas over Ni/Al2O3 in fluidized-and fixed-bed reactors [J], Catalysis today, 2002, 77(3), 181-189.
54. Bradford M C J, Vannice M A, CO_2 Reforming of CH_4 over Supported Pt Catalysts [J], Journal of Catalysis, 1998, 173(1), 157-171.
55. Souza M V M, Aranda D A G, Schmal M, Reforming of Methane with Carbon Dioxide over Pt/ZrO2/Al2O3 Catalysts [J], Journal of Catalysis, 2001, 204(2), 498-511.
56. Cai W, Wang F, Zhan E, et al, Hydrogen production from ethanol over Ir/CeO_2 catalysts: A comparative study of steam reforming, partial oxidation and oxidative steam reforming [J], Journal of Catalysis, 2008, 257(1), 96-107.

57. Zhao Y, Pan Y, Xie Y, et al, Carbon dioxide reforming of methane over glow discharge plasma-reduced Ir/Al_2O_3 catalyst [J], Catalysis Communications, 2008, 9(7), 1558-1562.

58. Iwasa N, Masuda S, Ogawa N, et al, Steam reforming of methanol over Pd/ZnO: effect of the formation of PdZn alloys upon the reaction [J], Applied Catalysis A: General, 1995, 125(1), 145-157.

59. Chin Y H, Dagle R, Hu J, et al, Steam reforming of methanol over highly active Pd/ZnO catalyst [J]. Catalysis Today, 2002, 77(1), 79-88.

60. Goula M A, Kontou S K, Tsiakaras P E, Hydrogen production by ethanol steam reforming over a commercial Pd/γ-Al_2O_3 catalyst [J], Applied Catalysis B: Environmental, 2004, 49(2), 135-144.

61. Craciun R, Daniell W, Knözinger H, The effect of CeO_2 structure on the activity of supported Pd catalysts used for methane steam reforming [J], Applied Catalysis A: General, 2002, 230(1), 153-168.

62. Kroll V C H, Swaan H M, Mirodatos C, Methane Reforming Reaction with Carbon Dioxide Over Ni/SiO_2 Catalyst: I. Deactivation Studies [J], Journal of Catalysis, 1996, 161(1),409-422.

63. Ruckenstein E, Hang Hu Y, Role of Support in CO_2 Reforming of CH4 to Syngas over Ni Catalysts [J], Journal of Catalysis, 1996, 162(2), 230-238.

64. Vaidya P D, Rodrigues A E, Kinetics of steam reforming of ethanol over a Ru/Al2O3 catalyst [J], Industrial & engineering chemistry research, 2006, 45(19), 6614-6618.

65. Qin D, Lapszewicz J, Study of mixed steam and CO_2 reforming of CH_4 to syngas on MgO-supported metals [J], Catalysis today, 1994, 21(2), 551-560.

66. Bradford M C J, Vannice M A, CO_2 Reforming of CH4 over Supported Ru Catalysts [J], Journal of Catalysis, 1999, 183(1), 69-75.

67. Rostrup-Nielsen J R, Catalytic steam reforming [M], Springer Berlin Heidelberg, 1984.

68. Richardson J T, Principles of catalyst development [M], New York: Plenum Press, 1989.

69. Schüth F, Hesse M, Unger K, Precipitation and coprecipitation [J], Handbook of heterogeneous catalysis, 1997.

70. Delmon B, Preparation of heterogeneous catalysts [J], Journal of Thermal Analysis and Calorimetry, 2007, 90(1), 49-65.

71. Goldstein J I, Newbury D E, Echlin P, et al,. Scanning electron microscopy and X-ray microanalysis. A text for biologists, materials scientists, and geologists [M], Plenum Publishing Corporation, 1981.

72. Engel A, Biological applications of scanning probe microscopes [J], Annual review of biophysics and biophysical chemistry, 1991, 20(1), 79-108.

73. Rostrup-Nielsen J R. Industrial relevance of coking [J], Catalysis Today, 1997, 37(3): 225-232.

74. Cheng F, Dupont V. Nickel catalyst auto-reduction during steam reforming of bio-oil model compound acetic acid [J]. International Journal of Hydrogen Energy, 2013, 38(35): 15160-15172.

75. Roy P S, Kang M S, Kim K. Effects of Pd–Rh Composition and $CeZrO_2$-Modification of Al_2O_3 on Performance of Metal-Foam-Coated Pd–Rh/Al_2O_3 Catalyst for Steam Reforming of Model Biogas [J]. Catalysis Letters, 2014, 144(12): 2021-2032.

76. Sprung C, Arstad B, Olsbye U. Methane Steam Reforming Over Ni/$NiAl_2O_4$ Catalyst: The Effect of Steam-to-Methane Ratio [J]. Topics in Catalysis, 2011, 54(16-18): 1063-1069.

77. Huo J, Jing J, Li W. Reduction time effect on structure and performance of Ni–Co/MgO catalyst for carbon dioxide reforming of methane [J]. International Journal of Hydrogen Energy, 2014, 39(36): 21015-21023.

78. Guczi L, Stefler G, Geszti O, et al. Methane dry reforming with CO_2: a study on surface carbon species [J]. Applied Catalysis A: General, 2010, 375(2): 236-246.

79. Junke X U, Wei Z, Jihui W, et al. Characterization and analysis of carbon deposited during the dry reforming of methane over Ni/La_2O_3/Al_2O_3 catalysts [J]. Chinese Journal of Catalysis, 2009, 30(11): 1076-1084.

80. Choudhary V R, Mondal K C, Mamman A S, et al. Carbon-free dry reforming of methane to syngas over $NdCoO_3$ perovskite-type mixed metal oxide catalyst [J]. Catalysis letters, 2005, 100(3-4): 271-276.

81. Iwarere S A, Rohani V J, Ramjugernath D, et al. Dry reforming of methane in a tip–tip arc discharge reactor at very high pressure [J]. International Journal of Hydrogen Energy, 2015, 40(8): 3388-3401.
82. Papadias D D, Lee S H D, Ferrandon M, et al. An analytical and experimental investigation of high-pressure catalytic steam reforming of ethanol in a hydrogen selective membrane reactor [J]. International Journal of Hydrogen Energy, 2010, 35(5): 2004-2017.
83. Takahashi Y, Yamazaki T. Behavior of high-pressure CH_4/CO_2 reforming reaction over mesoporous Pt/ZrO2 catalyst [J]. Fuel, 2012, 102: 239-246.
84. Li Z, Cai N. Modeling of multiple cycles for sorption-enhanced steam methane reforming and sorbent regeneration in fixed bed reactor [J]. Energy & Fuels, 2007, 21(5): 2909-2918.
85. Hirschfelder J O, Curtiss C F, Bird R B, et al. Molecular theory of gases and liquids [M]. New York: Wiley, 1954.
86. Xu J, Froment G F. Methane steam reforming, methanation and water-gas shift: I. Intrinsic kinetics [J]. AIChE Journal, 1989, 35(1): 88-96.
87. Richardson J T, Paripatyadar S A. Carbon dioxide reforming of methane with supported rhodium [J]. Applied Catalysis, 1990, 61(1): 293-309.

88. Prabhu A K, Liu A, Lovell L G, et al. Modeling of the methane reforming reaction in hydrogen selective membrane reactors [J]. Journal of membrane science, 2000, 177(1): 83-95.

Biographical Information

Xiao Zhang received his Bachelor Degree in Thermal Engineering from Huazhong University of Science and Technology, Wuhan, China in 2006. He started to pursue his PhD degree in Mechanical and Aerospace Engineering Department at the University of Texas at Arlington since 2009. His research interests mainly include experimental study on sustainable energy development. And his research area involves coal pyrolysis, Fisch-Tropsch synthesis and natural gas reforming.